

NACA RM A51K27

5-1



RESEARCH MEMORANDUM

CLASSIFICATION CHANGED TO Unclassified
BY AUTHORITY OF NASA Bull. # 73
ON 1/24/67 OF SEC

BODIES OF REVOLUTION FOR MINIMUM DRAG
AT HIGH SUPERSONIC AIRSPEEDS

By A. J. Eggers, Jr., David H. Dennis,
and Meyer M. Resnikoff

Ames Aeronautical Laboratory
Moffett Field, Calif.

ENGINEERING DEPT. LIBRARY
CHANCE-VOUGHT AIRCRAFT
DALLAS, TEXAS

~~CONFIDENTIAL~~
CLASSIFICATION

This material contains information affecting the National Defense of the United States within the meaning of the espionage laws, Title 18, U.S.C., Sections 793 and 794, the transmission or revelation of which in any manner to unauthorized person is prohibited by law.

NATIONAL ADVISORY COMMITTEE FOR AERONAUTICS

WASHINGTON
February 25, 1952

NATIONAL ADVISORY COMMITTEE FOR AERONAUTICS

RESEARCH MEMORANDUMBODIES OF REVOLUTION FOR MINIMUM DRAG
AT HIGH SUPERSONIC AIRSPEEDSBy A. J. Eggers, Jr., David H. Dennis,
and Meyer M. Resnikoff

SUMMARY

Approximate shapes of nonlifting bodies having minimum pressure foredrag at high supersonic airspeeds are calculated. With the aid of Newton's law of resistance, the investigation is carried out for various combinations of the conditions of given body length, base diameter, surface area, and volume. In general it is found that when body length is fixed, the body has a blunt nose; whereas, when the length is not fixed, the body has a sharp nose. In the case of a body of given length and base diameter, the additional effect of curvature of the flow over the surface is investigated to determine its influence on the shape for minimum drag. The effect is to increase the bluntness of the shape in the region of the nose and the curvature in the region downstream of the nose.

Several bodies of revolution of fineness ratios 3 and 5, including the calculated shapes of minimum drag for given length and base diameter and for given base diameter and surface area, were tested in the Ames 10- by 14-inch supersonic wind tunnel at Mach numbers from 2.73 to 5.00. A comparison of theoretical and experimental foredrag coefficients indicates that the calculated minimum-drag bodies are reasonable approximations to the correct shapes. It is verified, for example, that the body for a given length and base diameter has as much as 18 percent less foredrag than a cone of the same fineness ratio.

INTRODUCTION

The shapes of nonlifting bodies of revolution having minimum pressure drag at supersonic speeds have been the subject of numerous theoretical investigations. Kármán (reference 1) determined the shape of such a body (neglecting base drag) with given length and base diameter. Somewhat later Haack (reference 2), Ferrari (reference 3), Lighthill (reference 4), and Sears (reference 5) calculated body shapes having minimum pressure drag for various other given conditions using methods similar to those first employed by Karman. In all these investigations

the assumption of small perturbation, potential flow was made. It is to be expected, therefore, that the shapes obtained by these investigators are representative of minimum-drag body shapes of practical fineness ratios only at low supersonic Mach numbers.

Perhaps the first calculation of the shape of a body having minimum drag was made by Newton (reference 6) using a method analogous to the present day calculus of variations. Newton was concerned with determining the body of given length and base diameter having minimum resistance when moving at sufficiently high speeds to insure that the inertia forces are large compared to the elastic forces in the immersing fluid. Thus, as shown by Sanger (reference 7) and Epstein (reference 8), the law of resistance adopted by Newton approximates that (neglecting viscous forces) for hypersonic air flows. According to this law, the local resisting pressure is proportional to the square of the free-stream velocity component normal to the body surface. Legendre (see, e.g., reference 9) further investigated Newton's problem and concluded that if no restrictions were imposed on the variation of slope along the surface, a body having a meridian curve composed of jagged lines (sharp edges forward) could be constructed which, with this law of resistance, would have less drag than Newton's body. It may easily be deduced, however, that Newton's law of resistance would not be satisfied on the surface of Legendre's body since gas would be trapped in a number of regions along the jagged contour. It may be shown in fact that when this law of resistance is satisfied at the surface - in which case the surface angles must lie between 0 and $\pi/2$ radians - then Newton's body may be considered the minimum pressure drag body for the given conditions.

Aside from the investigations of Newton and Legendre, it appears that little, if any, work has been done which is applicable to the determination of body shapes which are especially suited, from the drag standpoint, to flight at high supersonic airspeeds. It has therefore been undertaken in the present report, using Newton's law of resistance and the calculus of variations, to determine body shapes having minimum pressure drag (neglecting base drag) at high supersonic speeds for various combinations of the conditions of given length, base diameter, surface area, and volume. In the case of a body of given length and base diameter, the effect of curvature of the flow over the surface is investigated to determine its influence on the shape for minimum drag.

Several bodies of revolution, including two of the bodies determined from this analysis, were tested at Mach numbers from 2.73 to 5.00 in the Ames 10- by 14-inch supersonic wind tunnel. Foredrag data at zero lift obtained from these tests are compared with the analytic predictions to assess the accuracy of the theoretical considerations.

SYMBOLS

- A local cross-sectional area of body
- a local speed of sound
- C_D drag coefficient $\left(\frac{4D}{q_0 \pi d^2} \right)$
- D pressure foredrag
- d maximum body diameter
- f integrand function
- I_D drag parameter $\left(\frac{D}{2\pi q_0} \right)$
- K hypersonic similarity parameter $\left(M_0 \frac{d}{l} \right)$
- l body length
- M Mach number $\left(\frac{U}{a} \right)$
- N distance measured normal to surface of body
- n exponent in equation defining shapes of experimental test bodies
- P pressure coefficient $\left(\frac{p - p_0}{q_0} \right)$
- p static pressure
- q dynamic pressure
- R radius of curvature of streamline in plane containing axis of symmetry (i.e., meridian plane) of body
- S body surface area
- U resultant velocity
- V body volume
- x,y coordinates of point on meridian curve of body (origin of coordinate system coincides with nose of body, and x axis coincides with axis of symmetry)

- γ ratio of specific heat at constant pressure to specific heat at constant volume
- δ angle (in meridian plane) between free-stream direction and tangent to body surface
- λ Lagrange multiplier
- ρ density

Subscripts

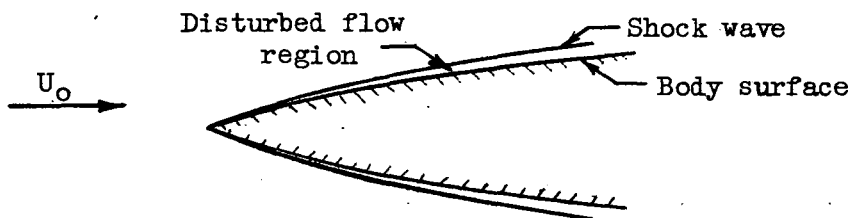
- o free-stream conditions
- 1 values at nose point of meridian curve
- 2 values at base point of minimizing curve
- + right-hand limiting value of quantity at corner on minimizing curve
- left-hand limiting value of quantity at corner on minimizing curve
- B values along meridian curve

THEORY

The investigation undertaken here is concerned with the shapes of nonlifting bodies of revolution having minimum pressure foredrag at high supersonic airspeeds. Difficulties inherent in the calculation of these shapes make it desirable to simplify the drag equation insofar as is practicable, consistent with retaining the salient features of the dependence of drag on body shape and free-stream conditions. Likewise, in view of the several conditions to be treated (viz., given length, base diameter, volume, and surface area), it is convenient to set up a procedure of analysis to fit the general problem at hand. These fundamental considerations will be discussed prior to the determination of specific minimum-drag shapes.

Fundamental Considerations

Simplified drag theory.— As pointed out in the introduction, Newton's law of resistance applies approximately to bodies traveling at high supersonic airspeeds. This observation has basis in the fact that at such speeds the inertia forces predominate over the elastic forces in the disturbed air. Thus, oblique shock flows approach the corpuscular-type flows treated by Newton as the Mach number of the free stream becomes large compared to 1. If it is further assumed that γ of the disturbed fluid approaches 1,¹ the shock-wave angle approaches the flow-deflection angle (see sketch). In this case the pressure



coefficient at a point just downstream of the wave is given by the simple expression (reference 8)

$$P = 2 \sin^2 \delta \quad (1)$$

This equation is recognized, of course, as being (aside from the constant multiplier) a mathematical statement of Newton's law of resistance for corpuscular or impact-type flow.

When the curvature of the body, and hence of the disturbed flow, is small in the stream direction, equation (1) should also predict the pressure coefficients at the surface of a body since, in this case, the centrifugal forces in the thin layer of air (sometimes referred to as the hypersonic boundary layer) between the shock and the surface should not appreciably alter the impact pressures. When the curvature of the body is large in the stream direction, centrifugal forces in the fluid between the shock and the surface may alter the pressures at the surface

¹This assumption was perhaps first suggested by Epstein (reference 8).

It has the advantage of simplifying the impact force analysis without significantly influencing its accuracy. In other words, these forces in flows about axially symmetric bodies are relatively insensitive to changes in γ from 1.4 to 1. Interestingly enough, present indications are that disturbed air flows in flight at extremely high Mach numbers will be characterized by values of γ below 1.4 (see references 10 and 11).

from those just downstream of the shock. Busemann (reference 12) investigated this problem and found that the pressure coefficient at a point on the surface of a body curved in the stream direction is given by the relation

$$P = 2 \left(\sin^2 \delta + \sin \delta \frac{d\delta}{dA} \int_0^A \cos \delta dA \right) \quad (2)$$

in the limit as $M \rightarrow \infty$ and $\gamma \rightarrow 1$.

In order to assess the accuracy with which the preceding equations may be expected to provide the pressure distributions, and thus pressure drags, on bodies operating at high supersonic airspeeds, the predictions of these equations are compared in figure 1 with those of the method of characteristics (obtained from reference 13) for an ogive operating at a value of the hypersonic similarity parameter K (ratio of free-stream Mach number to slenderness ratio) equal to 2, corresponding to a free-stream Mach number of 6. It is evident that the theory of Busemann (equation (2)) yields far too low pressures downstream of the nose, while the simple impact theory (equation (1)) is in reasonably good over-all agreement with the method of characteristics.² The relatively poor predictions of the Busemann theory are associated with the fact that it strongly overestimates centrifugal-force effects at free-stream Mach numbers which are large compared to 1, but for which γ of the air flow downstream of the bow shock is closer to 1.4 than 1 (i.e., at flow conditions of principal interest in this paper). This matter will be discussed in greater detail later in the paper. Agreement comparable to that just discussed is obtained with the other results presented in reference 13 for $K = 2$. For lower values of K the agreement of the impact theory with the method of characteristics is somewhat poorer, as would be expected; however, it does not become unacceptably poor except for values of K below 1 (e.g., the pressure coefficients differ by from 0 to 35 percent for a K of 1/2). It is therefore concluded that for values of K greater than 1, equation (1) may be used with acceptable accuracy for the purposes of this paper to predict the pressure distributions and thus pressure drags on bodies.³

²The characteristics solutions of reference 13 were carried out for $\gamma = 1.4$. Free flight at the larger values of K considered in this report would produce values of γ downstream of the bow shock slightly less than 1.4; however, the small decreases in γ would not significantly alter the results presented.

³The approximate theory of reference 14 might also be employed in an analysis of this type - this theory is, in fact, more accurate than those discussed, so long as the flow is everywhere supersonic. However, the theories considered here have the advantage, as will be apparent later, of predicting approximately correct values of surface pressures for arbitrarily large surface slopes.

For this reason, and because of its simplicity, it is employed throughout the subsequent analysis.

If the manner in which the pressure coefficient varies over the surface is known, it is a simple matter, of course, to evaluate the pressure drag of a body. Neglecting the base-drag contribution, we have then

$$D = \frac{C_D q_0 \pi d^2}{4} = 2\pi q_0 \int_0^l P y y' dx \quad (3)$$

where y' denotes the derivative dy/dx . This equation may be expressed in a form more convenient for use here

$$I_D = \frac{D}{2\pi q_0} = \int_0^l P y y' dx \quad (4)$$

If P in this expression is replaced by its value given in equation (1) (noting that $\sin^2 \delta = \frac{y'^2}{1+y'^2}$), there is then obtained the relation

$$I_D = \int_0^l \frac{2yy'^3}{1+y'^2} dx \quad (5)$$

It remains now to consider the procedure for employing this expression in combination with the methods of the variational calculus in order to determine the desired minimum-drag body shapes.

Procedure for Calculating Minimum-Drag Bodies

The calculation of minimum-drag body shapes of interest here is equivalent to determining the form of the function $y = y(x)$ which minimizes the integral defined in equation (5) for the various given conditions. In considering the procedure for carrying out this calculation, however, it is convenient, for reasons that will be apparent later, to write equation (5) in a form which effectively yields the total drag as the sum of the drag on any finite region of infinite slope at the nose plus the drag on the surface downstream of the nose. Thus we have

$$I_D = y_1^2 + \int_0^{x_2} \frac{2yy'^3}{1+y'^2} dx \quad (6)$$

where the variable limit x_2 is introduced to permit variations in body length. The conditions of given volume or given surface area are fixed by the auxiliary requirements that, respectively,

$$\frac{V}{\pi} = \int_0^{x_2} y^2 dx = \text{const.} \quad (7)$$

or (neglecting base area)

$$\frac{S}{2\pi} = \frac{y_1^2}{2} + \int_0^{x_2} y \sqrt{1 + y'^2} dx = \text{const.} \quad (8)$$

When the length and base diameter are given, the problem is simply to minimize the function I_D given by equation (6). However, according to the isoperimetric rule of the calculus of variations (see, e.g., reference 15), the problem of minimizing the function I_D , subject to the auxiliary condition given by equation (7) or (8), is equivalent to minimizing the new function J_D , where

$$J_D = I_D + \lambda \frac{V}{\pi} \quad (9)$$

or

$$J_D = I_D + \lambda \frac{S}{2\pi} \quad (10)$$

depending on whether the volume or surface area is given. The parameter λ is a constant, sometimes called the Lagrange multiplier.

With the aid of equations (6) through (10), the integrand functions to be minimized can be immediately written. These functions are as follows:

case a, given length and base diameter

$$f = \frac{2yy'^3}{1+y'^2} \quad (11)$$

case b, given volume and length or base diameter

$$f = \frac{2yy'^3}{1+y'^2} + \lambda y^2 \quad (12)$$

case c, given surface area and length or base diameter

$$f = \frac{2yy'^3}{1+y'^2} + \lambda y \sqrt{1+y'^2} \quad (13)$$

Now any function $y = y(x)$ which minimizes equation (6), (9), or (10) must, irrespective of the given conditions, satisfy the Euler equation (for zero first variation of I_D or J_D with small changes in the function $y(x)$)

$$\frac{d}{dx} f_{y'} - f_y = 0 \quad (14)$$

where $f_{y'}$ and f_y denote the partial derivatives $\frac{\partial f}{\partial y'}$ and $\frac{\partial f}{\partial y}$, respectively. Since the integrand functions given above are free of the independent variable, the first integral of the Euler equation for these functions follows immediately, namely,

$$y' f_{y'} - f = \text{const.} \quad (15)$$

Substituting, successively, equations (11), (12), and (13) into this equation there are then obtained the expressions

$$\frac{4yy'^3}{(1+y'^2)^2} = \text{const.} \quad (16)$$

$$\frac{4yy'^3}{(1+y'^2)^2} - \lambda y^2 = \text{const.} \quad (17)$$

and

$$y \left[\frac{4y'^3}{(1+y'^2)^2} - \frac{\lambda}{\sqrt{1+y'^2}} \right] = \text{const.} \quad (18)$$

for cases a, b, and c, respectively. Solutions to these differential equations satisfying the terminal conditions on the bodies are minimizing curves for the given conditions.

When the end points of a minimizing curve are not fixed, other terminal conditions must be imposed on the function $y = y(x)$. Thus, to determine the ordinate at the nose, it is required that (see reference 16)

$$\left(f_{y'} - \frac{d}{dy} y^2 \right) \Big|_{y=y_1} = 2y \frac{y'^2 - 1}{(1+y'^2)^2} \Big|_{y=y_1} = 0 \quad (19)$$

for cases a and b, while

$$\left[f_{y'} - \frac{d}{dy} \left(y^2 + \lambda \frac{y^2}{2} \right) \right] \Big|_{y=y_1} = y_1 \left[2 \frac{y'^4 + 3y'^2}{(1+y'^2)^2} + \frac{\lambda y'}{\sqrt{1+y'^2}} - (2+\lambda) \right] \Big|_{y=y_1} = 0 \quad (20)$$

for case c. Similarly, when the length is not given it is necessary that

$$\left(y' f_{y'} - f \right) \Big|_{x=x_2} = 0 \quad (21)$$

and when the base diameter is not given it is required that

$$f_{y'} \Big|_{x=x_2} = 0 \quad (22)$$

In addition to the above described conditions, two checks must be made to determine completely the shape of a minimizing curve. The first of these checks entails ascertaining whether there are any corners (between the end points) on the curve. This is accomplished by determining whether the function $y = y(x)$ can satisfy the requirement that (see reference 15)

$$f_{y'+} = f_{y'-} \quad (23)$$

at a point of discontinuity in y' . If this equation is not satisfied, no corners exist. The second check requires that the Legendre condition (for a positive second variation),

$$f_{y'y'} \geq 0 \quad (24)$$

be satisfied everywhere on the curve. With the aid of these checks, the minimizing curves for various combinations of the conditions of given length, base diameter, volume, and surface area can be uniquely defined. The calculation of these curves for several such combinations is now undertaken.

Calculation of Minimum-Drag Bodies

Given length and base diameter.— Equations (16) and (19) give the first integral to Euler's equation and the terminal condition at the nose, respectively, for these given conditions. It is evident upon examining these equations that the minimizing curve cannot, in general, pass through both the points $(0,0)$ and (x_2,y_2) , but must, in fact, have its forward termination point at $(0,y_1)$ with $y_1' = 1$. With this information, the minimizing curve can be represented in parametric form, namely,

$$\left. \begin{aligned} y &= \frac{y_1}{4} \frac{(1 + y'^2)^2}{y'^3} \\ x &= \frac{y_1}{4} \left(\frac{3}{4y'^4} + \frac{1}{y'^2} - \frac{7}{4} + \ln y' \right) \end{aligned} \right\} \quad (25)$$

It is easily shown with the solution to the Euler equation and equation (23) that there are no corners on the minimizing curve;⁴ thus the variation of y with x is readily determined with the relations of equation (25) for a given l and d (corresponding to a given x_2 and y_2) of a body. These relations for a body of given fineness ratio can be shown to be equivalent to those originally developed by Newton (see reference 6).

Given length and volume.— For these given conditions, the terminal conditions (equations (19) and (22)) require the slopes at the nose and at the base to be, respectively, $y_1' = 1$ and $y_2' = 0$. The first integral to the Euler expression (equation (17)) then leads to the following parametric representation of the minimizing curve:

$$\left. \begin{aligned} y &= \frac{2y'^3}{\lambda(1+y'^2)^2} + \sqrt{\left[\frac{2y'^3}{\lambda(1+y'^2)^2} \right]^2 - \frac{y_1 - \lambda y_1^2}{\lambda}} \\ x &= \int_{y_1}^y \frac{dy}{y'} \end{aligned} \right\} \quad (26)$$

⁴Similarly, it can be shown that there are no corners between $(0,y_1)$ and (x_2,y_2) on any of the minimizing curves to be treated here.

From the relations of equation (26) it is clear, again, that the minimizing curve cannot pass through (0,0), the condition $y_1' = 1$ determining a value $y_1 > 0$. These relations, together with the volume condition (equation (7)) and the given length condition, serve to determine y_1 and λ and thus, of course, the shape of the entire body. As the length approaches 0, λ becomes infinitely negative; while, as the length becomes infinitely large, λ approaches 0. (In the latter case the body shape approaches the minimum-drag shape for the given length and diameter condition, $l/d \rightarrow \infty$.) Intermediate negative values of λ correspond to intermediate values of length for a given volume.

Given length and surface area.— In this case a first integral to the Euler equation is given by equation (18), and the parametric representation of the minimizing curve may be written immediately in the form

$$\left. \begin{aligned} y &= \frac{\text{const. } (1+y'^2)^2}{4y'^3 - \lambda(1+y'^2)^{3/2}} \\ x &= \int_{y_1}^y \frac{dy}{y'} \end{aligned} \right\} \quad (27)$$

Upon examination of this equation and equations (20) and (22), it becomes apparent that, again, the minimizing curve cannot go through the point (0,0). The latter equations determine uniquely, however, the values of y_1' ($y_1' < 1$), and y_2' ($0 < y_2' < y_1'$), in terms of the parameter λ . Similarly, the length and surface-area condition in combination with the above equations determines the value of λ . Thus it is easily shown that the practical range of λ is from -2 to 0 (corresponding to body lengths of from zero to infinity for a given surface area — in the latter case the Newton body is again obtained).

Given base diameter and volume.— With these given conditions, the first integral to the Euler relation is given by equation (17), while the terminal conditions at the fore-and-aft ends of the body are fixed by equations (19) and (21), respectively. It is evident that the minimizing curve must, in general, pass through the origin in order to satisfy all these equations in addition to the Legendre condition (equation (24)). The shape of the minimizing curve may thus be defined parametrically as follows:

$$\left. \begin{aligned} y &= \frac{4}{\lambda} \frac{y_1'^3}{(1+y_1'^2)^2} \\ x &= \frac{2}{\lambda} \frac{y_1'^4 + 3y_1'^2}{(1+y_1'^2)^2} \end{aligned} \right\} \quad (28)$$

where $y_1' = 0$. Combining this expression with equation (7), there is then obtained for the volume of the body

$$V = \frac{\pi y_2^3}{120 y_2'} (y_2'^4 + 6y_2'^2 + 45) \quad (29)$$

The range of λ for which these results are applicable⁵ is from zero to $3\sqrt{3}/4y_2$, corresponding to a volume range from infinity to $\pi y_2^3 \sqrt{3}/5$. For a given y_2 and a given $V > \pi y_2^3 \sqrt{3}/5$ (corresponding to $\frac{l}{d} > \sqrt{3}/2$), equation (29) has two solutions in y_2' . One solution yields values of y_2' greater than $\sqrt{3}$, which result violates the Legendre condition (see equation (24)), while the other yields permissible values less than $\sqrt{3}$. When y_2 and y_2' are known, λ may then be determined from the first relation of equation (28), namely,

$$\lambda = \frac{4}{y_2} \frac{y_2'^3}{(1+y_2'^2)^2} \quad (30)$$

The determination of y and x follows directly, of course, from equation (28).

Given base diameter and surface area.— In this case equations (18), (20), and (21) determine the shape of the minimizing curve as being simply a straight line

$$y = x \sqrt{\frac{(\lambda/4)^{2/3}}{1 - (\lambda/4)^{2/3}}} \quad (31)$$

where the parameter λ is given by the equation

⁵The solution given here is not applicable to bodies of extremely small fineness ratios (viz., $\frac{l}{d} < \frac{\sqrt{3}}{2}$) as can be easily deduced from equation (28).

$$\lambda = 4 (\pi y_2^2 / S)^3 \quad (32)$$

Thus, the minimum-drag body for given base diameter and surface area is a cone.

Comparison of Minimum-Drag Body Shapes

The previous calculation of minimum-drag bodies reveals two general characteristics of their shapes; namely, when the length is given (fixed) the bodies assume blunt noses, whereas, when the length is not given (i.e., is free), the bodies assume sharp noses. The former characteristic may be traced to the fact that with the length restricted, the net drag is reduced by accepting higher pressures on a relatively small area of large slope near the nose, thus achieving lower pressures on a relatively large area of small slope near the base. On the other hand, when the length is not restricted it is evident that a sharp rather than a blunt nose will obtain for minimum drag, since the drag of any blunt-nosed body can be reduced by simply relaxing the requirement on length, thereby allowing the body to be made sharp nosed and generally more slender.

In order to permit a quantitative comparison of the shapes of the calculated minimum-drag bodies, typical meridian curves for these bodies are shown in figure 2. For simplicity the bodies are compared on the basis of the same fineness ratio - ordinates have been plotted to an expanded scale to better indicate the relative shapes. The maximum bluntness is evidently obtained when the drag is minimized for a given length and surface area, while the maximum sharpness (a cusp nose) is obtained when the base diameter and volume are given. It is apparent from figure 2 that the flat-nosed portions of the meridian curves for the given length bodies are in all cases very small. For example, y_1 equals $0.0050y_2$ for the body of given length and volume. On the basis of several calculations it is indicated, as might be expected, that the degree of bluntness will increase with decreasing fineness ratio.

It is also of interest to compare minimum-drag body shapes determined with the aid of the linear theory (see, e.g., reference 2) with those found using the impact theory, that is, bodies especially suited for flight at low and high supersonic speeds, respectively. Such a comparison is shown in figure 3 for the case of given length and base diameter. It is seen that qualitatively the shapes are similar although the minimum-drag body for low supersonic speeds is generally the fatter

of the two.⁶ Comparisons of the results of this paper with those of reference 2 for other given conditions also indicate qualitative agreement as to general body shapes despite the marked difference in the laws governing the surface pressures.

All the preceding analysis has been predicated on the assumption that the flow of air at high supersonic speeds may, insofar as pressure forces are concerned, be approximated by a Newtonian-type flow. It remains now to test the accuracy of this assumption and other aspects of the analysis by experiment.

EXPERIMENT

It has been undertaken to obtain a partial check on the findings of the preceding theoretical analysis by determining experimentally the foredrags on a family of bodies, including calculated minimum-drag shapes, at Mach numbers from 2.7 to 5.0. The analysis may be expected to apply at least approximately in this range since the corresponding values of the hypersonic similarity parameter K were, for the most part, greater than 1. A brief description of these tests is presented.

Test Apparatus

Wind tunnel.—The tests were conducted in the Ames 10- by 14-inch supersonic wind tunnel which is a closed test section, nonreturn tunnel of the continuous-flow type. A schematic view of the wind tunnel and auxiliary equipment is shown in figure 4. The 10-inch dimension corresponds to the width of the tunnel which is constant from just upstream of the nozzle to downstream of the diffuser. The 14-inch dimension is the nominal value of the depth of the test section. The top and bottom walls of the wind tunnel are rigid (as are the sidewalls) and form the nozzle and the converging-diverging diffuser. These walls are translated and/or rotated relative to each other during operation of the tunnel in order to vary the test-section Mach number. At the same time the diffuser shape is adjusted to decrease the intensity of the terminal shock system, thus decreasing the power required to operate the tunnel.

⁶Part of this difference in shapes may stem from the fact that the body derived using linear theory was required to have zero slope at the base. Also, as will be shown later, the true minimum-drag shape at high supersonic airspeeds may be somewhat fatter than that obtained using impact theory, due to the fact that centrifugal forces are neglected in this theory.

At present the tunnel is operated at test Mach numbers from 2.7 to 5.0; operation at higher Mach numbers is prohibited by excessive condensation of the air in the test section.

Flow in the diverging portion of the diffuser is stabilized by removing part of the low-energy boundary-layer air through scoops located at the minimum section of the diffuser. This air is diverted to the vacuum pumps shown beneath the wind tunnel in figure 4. The remainder of the air is exhausted either directly to the atmosphere, or, when higher pressure ratios are required, through the air-driven, two-stage, centrifugal-evacuator system shown at the lower right of figure 4.

Supply air for the wind tunnel and drive air for the centrifugal evacuators are provided by two stages of centrifugal compressors (not shown in fig. 4) at absolute pressures up to a maximum of 6 atmospheres. The supply air is passed through coolers and silica-gel dryers to reduce the absolute humidity to less than 0.0001 pound of water per pound of dry air. The drive air is piped to the evacuators from immediately downstream of the second stage compressors.

The schlieren apparatus used for visual investigations of the flow is shown schematically in figure 4. The system consists basically of a light source, a spherically ground mirror with a radius of curvature of 50 feet, an adjustable knife edge, and a ground glass viewing screen which may be replaced by photographic film packs. Two plane mirrors are used to reduce the length of the system while retaining the 50-foot light path. The entire apparatus is installed in a light-tight enclosure straddling the tunnel test section. The test section is traversed twice by the light beam, thus increasing the sensitivity over that of the more conventional types of schlieren systems.

The schlieren apparatus discussed previously was converted to a shadowgraph system for the tests reported here in order to obtain clearer outlines of the bow shock waves which were of primary interest. This conversion was accomplished by simply replacing the spherical mirror in the schlieren system with photographic plates and operating the light source as a spark - in this case the test section is traversed only once, of course, by the light beam.

In figure 5 are shown the variations in Mach number along the test-section center line as determined from pitot and static pressure measurements made at 1.5-inch intervals in the axial direction. These variations do not exceed ± 0.02 except at Mach numbers of 4 and 5 where they amount to ± 0.03 and ± 0.04 , respectively. The corresponding maximum variations in pressure coefficient are ± 0.005 , 0.003, and 0.002, respectively.

The variation of Reynolds number per foot with Mach number for the present tests is shown in figure 6.

Instrumentation.— Aerodynamic drag was measured by a single-component strain-gage balance. A cutaway drawing of the balance is shown in figure 7. Tare forces on the sting supporting the model were eliminated by enclosing the sting within a shroud that extended to within 0.040 inch of the model base.

Pressures at the model base were determined with the aid of a low-pressure McLeod gage. Stagnation pressures in the reservoir were measured on a Bourdon-tube gage.

Models.— Five models of fineness ratio 3, and three models of fineness ratio 5 were tested. With the exception of an $l/d = 3$ tangent ogive (this shape was included as being typical of those in common usage), all models had meridian section shapes given by the equation

$$\frac{y}{d/2} = \left(\frac{x}{l}\right)^n \quad (33)$$

where n was given values of 1, $3/4$, $1/2$, and $1/4$. When $n = 3/4$, the body shapes defined by the above expression closely approximate the minimum-drag shapes for given length and base diameter (equation (25))⁷ for $l/d = 3$ and 5 (see fig. 8).

When $n = 1$, the cone is, of course, obtained which is the minimum-drag body for a given base diameter and surface area. Minimum-drag shapes for two different given conditions are thus included among the bodies tested.

Photographs of the eight models tested are shown in figure 9. The $l/d = 3$ bodies (fig. 9(a)) are, from left to right in the photograph, the cone, $3/4$ -power body, $1/2$ -power (parabolic) body, $1/4$ -power body, and the tangent ogive which has a profile section radius of curvature of 9.25 body diameters. From left to right in figure 9(b) are the $l/d = 5$ cone, $3/4$ -power body, and $1/2$ -power body. The base diameter of all models was 1 inch.

⁷The accuracy of this approximation increases with increasing values of l/d as can easily be seen upon examination of equation (25).

Accuracy of Test Results

The accuracy of the foredrag coefficients is effected by uncertainties in the measurements of the following quantities: stagnation pressures, free-stream pitot pressures, free-stream static pressures, base pressures, and the forces on the models as measured by the strain-gage balance.

Both static and free-stream dynamic pressures were determined from wind-tunnel calibration data and stagnation-pressure readings. The latter measurements were accurate to within $\pm 1/2$ percent, thus static and dynamic pressures are uncertain by this amount plus possible calibration errors of ± 1 percent over the Mach number range of the tests. The uncertainty in foredrags due to inaccuracies in the determination of base pressures does not exceed ± 1 percent.

Because of the small drag forces measured, the source of greatest error was the strain-gage balance system. The uncertainty in drag due to zero shifts, thermal effects, and friction varied from approximately ± 2 percent at the lower Mach numbers to ± 6 percent at the highest Mach numbers.

The models were tested on the tunnel center line between stations 46 and 54. In this region the variations in stream static pressure coefficient discussed previously were too small to warrant the application of a bouyancy correction to the measured drags.

The combined effects of all the sources of error result in probable uncertainties in measured foredrag coefficients of from ± 0.001 at the low Mach numbers to ± 0.005 at a Mach number of 5.0.⁸

In order to reduce this error in the data presented here, particularly at the higher Mach numbers, several measurements were made at each Mach number and the average values of foredrag coefficients were employed.

RESULTS AND DISCUSSION

The variations with Mach number of the pressure drag and skin-friction drag for cones with laminar boundary layers can be accurately

⁸At Mach numbers near 5 there is some additional uncertainty due to the presence of a small amount of condensed vapor (including O_2 and N_2) in the test-section air stream; however, as will be evident later, this uncertainty is inconsequential to the present tests.

predicted with available theories. The Reynolds numbers of the present tests were sufficiently low to insure laminar boundary layers in all cases (see fig. 10 showing sharply defined boundary layers in shadowgraphs of the flow about the $l/d = 3$ cone and $1/2$ -power body). Since such a calculation provides a reliable check on the accuracy of the experimental results of the present tests, it has been carried out for the cone of $l/d = 3$. The pressure drag was determined from reference 17. The skin-friction drag for a flat plate was determined from the results of reference 18 and modified by the transformation of Hantzche and Wendt (reference 19) for the case of the cone. A comparison of the foredrag coefficients for this cone as determined experimentally and by the calculations described above is shown in figure 11. Good agreement between experiment and this relatively exact theory is observed over the Mach number range of the tests, thus substantiating the accuracy of the experiments. The increase in foredrag coefficients at Mach numbers above 4.5 is due to the increase in friction drag which in turn results from the rapid decrease in Reynolds number with increasing Mach number in this range (see fig. 6).

The variations with Mach number of the foredrag coefficients of the eight test bodies are shown in figure 12. With the exception of the $1/4$ -power body, these variations are similar to those for the fineness ratio 3 cone previously discussed. In the case of the $1/4$ -power body C_D increases with increasing Mach number over the entire test range. This behavior may result from the fact that, while the skin-friction drag coefficient is increasing with Mach number, the pressure drag coefficient for this very blunt body, in contrast to the more slender bodies investigated, probably decreases little if at all.⁹

The results presented in figure 12 show that, as predicted in the analysis, the $3/4$ -power bodies have the minimum foredrags of all bodies tested having the same fineness ratios. Percentagewise the improvement is larger at the higher Mach numbers. This result might be anticipated from the simplified drag theory used in the analysis (this theory is strictly applicable only at high Mach numbers for which the value of the hypersonic similarity parameter K for the flow is greater than 1). Except in the case of the bluntest body, however, the simplified theory yields foredrags that are appreciably lower than those obtained experimentally at all Mach numbers. Nor would the addition of the correct skin-friction drag to the theoretical pressure drag bring theory and experiment into agreement since the theoretical drag is generally too low. The differences between the experimental and theoretical results are illustrated in the following table where the drag coefficients are compared for all the bodies at a free-stream Mach number of 4.0.

⁹In the limit as the body becomes completely blunt, that is, a cylinder, the pressure drag coefficient increases slightly with increasing Mach number in this range.

Model	Foredrag coefficients	
	Experiment	Equation 1
$l/a = 3$ first power (cone)	0.079	0.0541
$l/a = 3$ $3/4$ power	.067	.0455
$l/a = 3$ $1/2$ power	.085	.0692
$l/a = 3$ $1/4$ power	.249	.2878
$l/a = 3$ ogive	.096	.0705
$l/a = 5$ first power (cone)	.043	.0198
$l/a = 5$ $3/4$ power	.037	.0167
$l/a = 5$ $1/2$ power	.046	.0300

At higher Reynolds numbers and higher Mach numbers corresponding to larger values of K (the highest value of K in the present tests was 1.67) it would be expected that theoretical and experimental foredrag coefficients would be in better agreement.

A check on the over-all accuracy with which the optimum shapes are predicted by the analysis is obtained by comparing theoretical and experimental values of the relative foredrag coefficients of the test bodies. Such a comparison is given in figure 13 where the ratios of the foredrag coefficients of a test body to the corresponding coefficients of the cone of the same fineness ratio are shown as a function of the exponent n in equation (33) defining the shapes of the test bodies. The theoretical predictions of the impact theory appear to be in good agreement with the experimental results at the higher values of n (approximately $n > 0.6$). Thus it is suggested that the $3/4$ -power body is a reasonable approximation to the correct minimum foredrag shape of given fineness ratio. At the lower values of n , however, it is indicated that in contrast to absolute drag, previously discussed, the relative drag is significantly overestimated by this theory. This result is not entirely surprising since the theory neglects centrifugal-force effects in the disturbed flow, and these effects must appreciably alter the pressures over the highly curved noses of the blunter bodies (see fig. 9).

As discussed earlier, the Busemann theory for infinitely high Mach numbers overestimates these effects at the Mach numbers of interest here. It has therefore been undertaken in appendix A of this paper to obtain a better estimate of centrifugal forces by accounting approximately for the decrease in these forces (at finite but high Mach numbers) associated with the increase in the lateral extent of the disturbed flow field with increasing distance downstream from the nose of the body (see fig. 10). The predictions of the modified impact theory shown in

figure 13 were obtained with the aid of this estimated centrifugal-force effect (see equation (A9)) in combination with equations (1) and (3). It is indicated that this theory is markedly superior to the impact theory at the lower values of n , corresponding to the blunter bodies, over the test Mach number range. The estimate of the centrifugal forces would thus appear to be in fair agreement with the actual magnitude of these forces.

It is also indicated in figure 13 that at the highest test Mach numbers (hence highest values of K) the modified theory is generally somewhat superior to the impact theory. This result suggests that improved approximations to the correct minimum-foredrag shapes for values of K appreciably greater than 1 may be obtained by using this theory rather than the simple impact theory. As a first step in the direction towards obtaining these shapes, the minimum-drag body of given length and base diameter has been calculated with the aid of the modified impact theory. This calculation is carried out in appendix B, and the resulting shape for a given fineness ratio is shown in figure 14. Newton's body of the same fineness ratio is also shown for comparative purposes and, as would be expected, this body is somewhat less blunt than the former shape in the region of the nose and has less curvature in the region downstream of the nose since centrifugal relieving effects on the surface pressures are not considered by the impact theory.

CONCLUDING REMARKS

It has been undertaken in this report to determine approximately the shapes of several bodies having minimum pressure foredrag at high supersonic airspeeds. With the aid of Newton's law of resistance and the calculus of variations, an investigation was carried out for various combinations of the conditions of given body length, base diameter, surface area, and volume. In general, it was found that when the length is fixed, the body has a blunt nose (i.e., a finite area of infinite slope at the nose) as in the classical problem considered by Newton; whereas when the length is not fixed the body has a sharp nose.

Several bodies of revolution of fineness ratios 3 and 5, including the calculated minimum-drag bodies for given length and base diameter and for given base diameter and surface area, were tested at Mach numbers from 2.73 to 5.00 in the Ames 10- by 14-inch supersonic wind tunnel. A comparison of the relative theoretical and experimental fore-drag coefficients indicated that the calculated minimum-drag bodies were reasonable approximations to the correct shapes. It was verified, for example, that the body for a given length and base diameter has as much as 18 percent less foredrag than a cone of the same fineness ratio.

The cone is, however, the calculated minimum-drag body for a given base diameter and surface area.

The comparison between theory and experiment also indicated that the centrifugal forces in the flow about bodies curved in the stream direction may significantly influence their drag. The relative extent of this influence was found to be predictable, particularly at the higher Mach numbers, with a simple modification to the impact theory of Newton. It was therefore suggested that improved approximations to minimum foredrag shapes at high supersonic airspeeds (for which the hypersonic similarity parameter has a value appreciably greater than 1) may be calculated with the aid of the modified impact theory. Such a calculation was carried out for the body of given length and base diameter. The resulting shape was found to be somewhat blunter in the region of the nose, and to have more curvature in the region downstream of the nose than the corresponding shape obtained using the simple impact theory.

Ames Aeronautical Laboratory,
National Advisory Committee for Aeronautics,
Moffett Field, Calif.

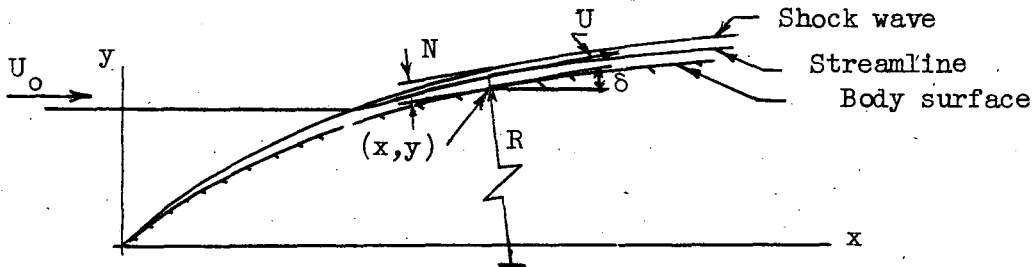
APPENDIX A

ESTIMATED EFFECT OF CENTRIFUGAL FORCES

ON SURFACE PRESSURE COEFFICIENTS

An estimate of the effect of centrifugal forces on the pressures at the surface of a body operating at high but finite Mach numbers may be obtained by comparing the disturbance flow fields at these Mach numbers with that associated with infinitely large Mach number.

At high Mach numbers the disturbed air flows in a relatively thin region (sometimes termed the hypersonic boundary layer) between the bow shock wave and the surface of the body (see sketch).



The change in pressure from the surface to the shock due to centrifugal forces in the fluid is given by the equation

$$\Delta p = \int_0^N \frac{dp}{dN} dN = \int_0^N \frac{\rho U^2}{R} dN$$

assuming the directions of the normals to the streamlines between the surface and the shock do not differ appreciably from the direction of the normal to the surface. This expression is more conveniently written in the form

$$\Delta p = \frac{\bar{U}}{\bar{R}} \int_0^N \rho U dN \tag{A1}$$

where \bar{U} and \bar{R} are mean values of the velocity and radius, respectively, in the interval N . Now the mass m of air between the surface and the shock flowing (in unit time) by a point on the body is given by the relation

$$m \approx 2\pi y \int_0^N \rho U dN \approx \pi y^2 \rho_0 U_0 \tag{A2}$$

Combining equations (A1) and (A2) there is then obtained for the pressure change

$$\Delta p = \frac{\bar{U}}{R} \frac{y}{2} \rho_0 U_0$$

or in coefficient form

$$\Delta P = \frac{\Delta p}{q_0} = \frac{y}{R} \frac{\bar{U}}{U_0} \quad (A3)$$

Now in the limit as the Mach number approaches infinity and γ of the disturbed fluid approaches 1, the thickness of the layer becomes infinitesimal and hence

$$\bar{R} = R_B \quad (A4)$$

Similarly, it is easily shown (e.g., with the compatibility equations applying along characteristic lines in axially symmetric supersonic flow) that

$$dU = 0$$

along any streamline downstream of the bow shock, and thus that

$$\bar{U} = \frac{2U_0}{y^2} \int_0^y y \cos \delta \, dy \quad (A5)$$

Hence, in this limiting case, equation (A3) takes on a form equivalent to that first deduced by Busemann (see second term on right of equation (2)), and later derived in reference 20, namely,

$$\Delta P = \frac{2}{R_B y} \int_0^y y \cos \delta \, dy \quad (A6)$$

where

$$\frac{1}{R_B} = \sin \delta \frac{d\delta}{dy}$$

On the other hand when the Mach number is finite, but high, and γ of the disturbed fluid is closer to 1.4 than 1, the preceding evaluations of \bar{R} and \bar{U} are in considerable error since the hypersonic boundary layer, although thin, is no longer of infinitesimal thickness. This change in the boundary layer results from the fact that the bow shock is detached (except perhaps at the nose) from the surface of the

body, the lateral distance from the surface to the shock increasing with increasing distance downstream from the nose (see sketch). Thus, for example, \bar{R} would be expected to approach R_B only near the nose, while with increasing distance downstream of the nose it would be expected to become larger than R_B . From the pressure distributions presented in reference 13 it is indicated, in fact, that for $K > 1$ (the range of K 's of interest in this paper) $\bar{R} \gg R_B$ near the maximum ordinate of the body. (This indication follows from the small values of the pressure coefficients near the maximum ordinate.) It is suggested, therefore, that at the high supersonic speeds under consideration, an approximation to \bar{R} is given by the relation

$$\frac{\bar{R}}{R_B} = \frac{1}{1 - \frac{y}{y_2}} \quad (A7)$$

Similarly, in the case of \bar{U} it no longer follows that the magnitude of the velocity must be constant along streamlines downstream of the bow shock since pressure disturbances can now be transmitted across streamlines. Thus a better first approximation to \bar{U} than that given by equation (A5) may be obtained from the simple corpuscular or impact theory,¹⁰ namely,

$$\bar{U} = U_0 \cos \delta \quad (A8)$$

Combining equations (A3), (A7), and (A8), the estimated change in pressure coefficient at the surface of a body due to centrifugal forces in high supersonic speed flow is obtained in the form

$$\Delta P = \frac{y}{R_B} \left(1 - \frac{y}{y_2}\right) \cos \delta$$

or

$$\Delta P = \frac{y}{2} \left(1 - \frac{y}{y_2}\right) \frac{d}{dy} (\sin^2 \delta) \quad (A9)$$

¹⁰With this theory, acceleration of the flow along a streamline is qualitatively accounted for.

APPENDIX B

CALCULATION OF MINIMUM-DRAG BODY OF GIVEN LENGTH AND
BASE DIAMETER, WITH CONSIDERATION OF CENTRIFUGAL
FORCES IN THE DISTURBED FLOW FIELD

For the purpose of this calculation, equations (1) and (A9) for the pressure coefficient are combined with equation (4) to yield the drag parameter in the form

$$I_D = y_1^2 + \varphi(y_1) + \int_0^{x_2} \left[2 \sin^2 \delta + \frac{y}{2} \left(1 - \frac{y}{y_2}\right) \frac{d}{dy} \sin^2 \delta \right] yy' dx \quad (B1)$$

The term y_1^2 represents the drag on any finite region of infinite slope at the nose, while the function $\varphi(y_1)$, given by¹¹

$$\varphi(y_1) = -\frac{y_1^2}{2} \left(1 - \frac{y_1}{y_2}\right) \cos^2 \delta_1$$

represents a "leading-edge thrust" due to the acceleration of the air flow about a corner (if it exists) at $(0, y_1)$.

The expression (B1) may be put in the form

$$I_D = y_1^2 + \int_0^{x_2} \left\{ \left[2 \sin^2 \delta + \frac{y}{2} \left(1 - \frac{y}{y_2}\right) \frac{d}{dy} \sin^2 \delta \right] yy' - \frac{d}{dx} \varphi(y) \right\} dx$$

whereupon (recalling $\sin^2 \delta = \frac{y'^2}{1+y'^2}$) the integrand simplifies to a function f given by the relation

¹¹This function may be obtained by evaluating

$$\lim_{\epsilon \rightarrow 0} \int_{y_1 - \epsilon}^{y_1 + \epsilon} \frac{y^2}{2} \left(1 - \frac{y}{y_2}\right) \frac{d}{dy} (\sin^2 \delta) dy$$

along the body-surface streamline about the corner at $(0, y_1)$.

$$f = yy' \left(2 - \frac{1 + \frac{3}{2} \frac{y}{y_2}}{1 + y'^2} \right)$$

With the aid of this expression and equations (15) and (19) the parametric representation of the minimizing curve can be obtained in the form

$$\left. \begin{aligned} y &= \frac{y_2}{3} \left[-1 + \sqrt{1 + \frac{15y_2'^3 (1+y'^2)^2}{(1+y_2'^2)^2 y'^3}} \right] \\ x &= \int_{y_1}^y \frac{dy}{y'} \end{aligned} \right\} \quad (B2)$$

where

$$y_1' = 1$$

and in general

$$y_1 \neq 0$$

The minimizing curve given by these relations, similar to the curve obtained from the impact pressure treatment, does not have a corner between the points $(0, y_1)$ and (x_2, y_2) . The minimum-drag shape defined by equation (B2) is compared in figure 14 with that determined earlier by considering impact pressures only.

REFERENCES

1. von Kármán, Th.: The Problem of Resistance in Compressible Fluids. GALCIT Pub. No. 75, 1936. (From R. Acad. D'Italia, vol. XIV, Roma, 1936)
2. Haack, W.: Projectile Forms of Minimum Wave Resistance. (Translation) Douglas Aircraft Company, Inc., Rept. 288, 1946.
3. Ferrari, Carlo: The Determination of the Projectile of Minimum Wave Resistance. Reale Accademia della Scienze de Torino Atti, 1939. (Issued as British, M.A.P. RTP Tr. 1180)
4. Lighthill, M. J.: Supersonic Flow Past Bodies of Revolution. R. & M. No. 2003, British A.R.C., 1945.
5. Sears, William R.: On Projectiles of Minimum Wave Drag. Quart. App. Math., vol. IV, no. 4, Jan. 1947, pp. 361-366.
6. Newton, Isaac: Principia - Motte's Translation Revised. Univ. of Calif. Press, 1946, pp. 333, 657-661.
7. Sanger, Eugene: Raketen-flugtechnik. R. Oldenbourg (Berlin), 1933, pp. 120-121.
8. Epstein, P. S.: On the Air Resistance of Projectiles. Proceedings of National Academy of Sciences, 1931, vol. 17, pp. 532-547.
9. Forsyth, A. R.: Calculus of Variations. The Cambridge Univ. Press (England), 1927, pp. 320-324.
10. Bethe, H. E., and Teller, E.: Deviations from Thermal Equilibrium in Shock Waves. Ballistic Research Laboratory Rep. No. X-117, Aberdeen Proving Ground, Aberdeen, Md., 1945.
11. Eggers, A. J., Jr.: One-Dimensional Flow of an Imperfect Diatomic Gas. NACA Rep. 959, 1950. (Formerly NACA TN 1861)
12. Busemann, A.: Flüssigkeits- und Garbewegung. Handwörterbuch der Naturwissenschaften. Gustav Fischer, Zweite Auflage, Jena, 1933.
13. Rossow, Vernon J.: Applicability of Hypersonic Similarity Rule to Pressure Distributions Which Include the Effects of Rotation for Bodies of Revolution at Zero Angle of Attack. NACA 2399, 1951.

14. Eggers, A. J., Jr., and Savin, Raymond C.: Approximate Methods for Calculating the Flow About Nonlifting Bodies of Revolution at High Supersonic Airspeeds. NACA TN 2579, 1951.
15. Bolza, Oskar: Lectures on the Calculus of Variations. G. E. Stechert and Co., New York, 1946 (1904 edition), pp. 22, 27, 38, 40, and 47.
16. Courant, R., and Hilbert, D.: Methoden der Mathematische Physik. J. Springer (Berlin), vol. 1, 1929, pp. 179-180.
17. Massachusetts Institute of Technology, Dept. of Elect. Engr., Center of Analysis. Tables of Supersonic Flow Around Cones, by the staff of the Computing Section, Center of Analysis, under the direction of Zdenek Kopal. (Tech. Rep. No. 1.) Cambridge, 1947.
18. Monaghan, R. J.: An Approximate Solution of the Compressible Laminar Boundary Layer on a Flat Plate. Tech. Note No. Aero 2025, Sup. 96, R.A.E. (British), 1949.
19. Hantzsche, W., and Wendt, H.: The Laminar Boundary Layer of a Circular Cone in Supersonic Flow at Zero Angle of Attack. (Die Laminare Grenzschicht bei einem mit Überschallgeschwindigkeit angeströmten nichtangestellten Kreiskegel. Jahrbuch der Deutschen Luftfahrtforschung, 1941, pt. I, pp. 76-77.) Translated by Ronald Kay, ed. by M. W. Rubesin. Engr. Res. Proj., Univ. Calif., Berkeley, Calif., May 1, 1947.
20. Ivey, H. Reese, Klunker, E. Bernard, and Bowen, Edward N.: A Method for Determining the Aerodynamic Characteristics of Two- and Three-Dimensional Shapes at Hypersonic Speeds. NACA TN 1613, 1948.

Page intentionally left blank

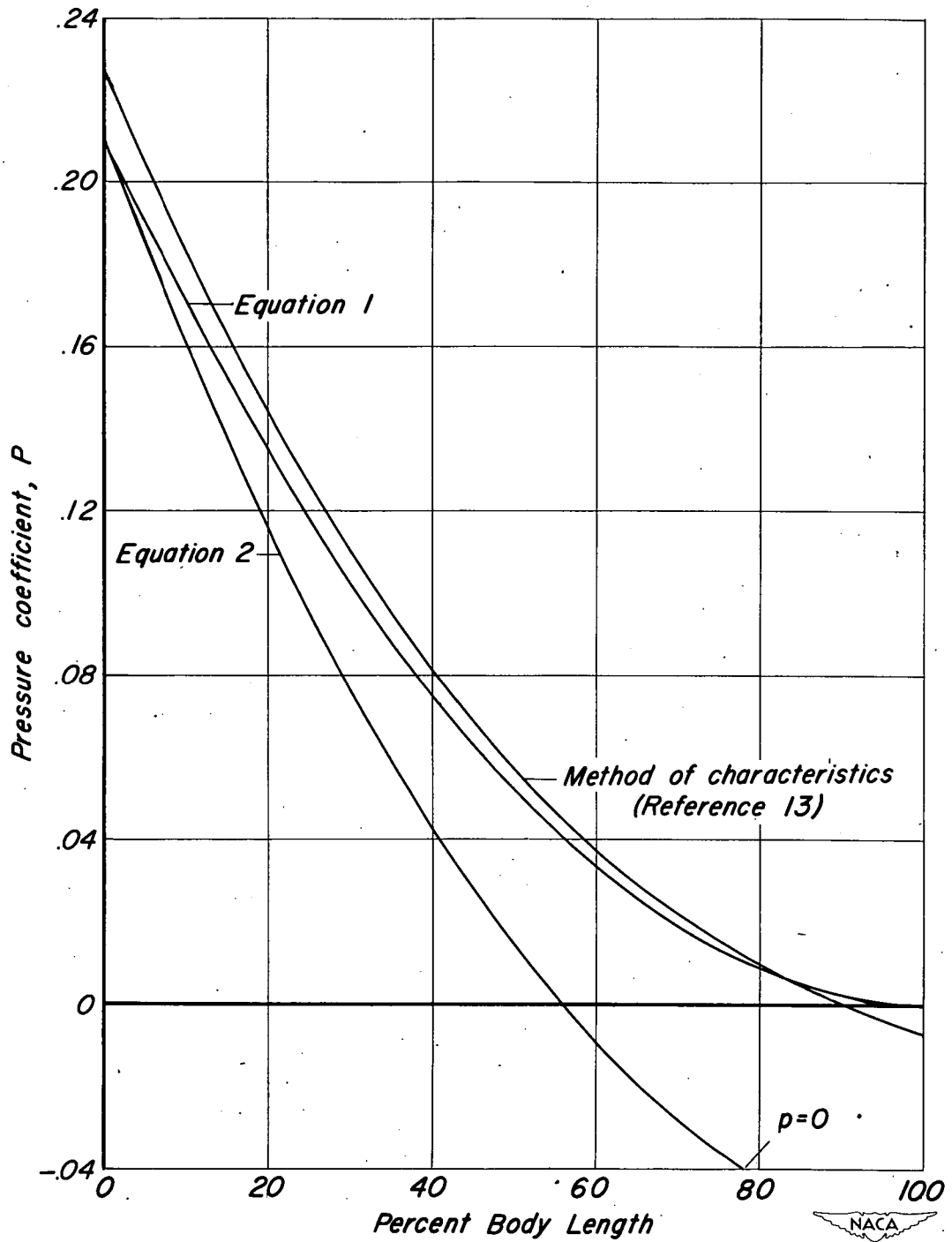


Figure 1.- Comparison of approximate and exact pressure distributions over a tangent ogive of fineness ratio 3 operating at a Mach number of 6 ($K=2$).

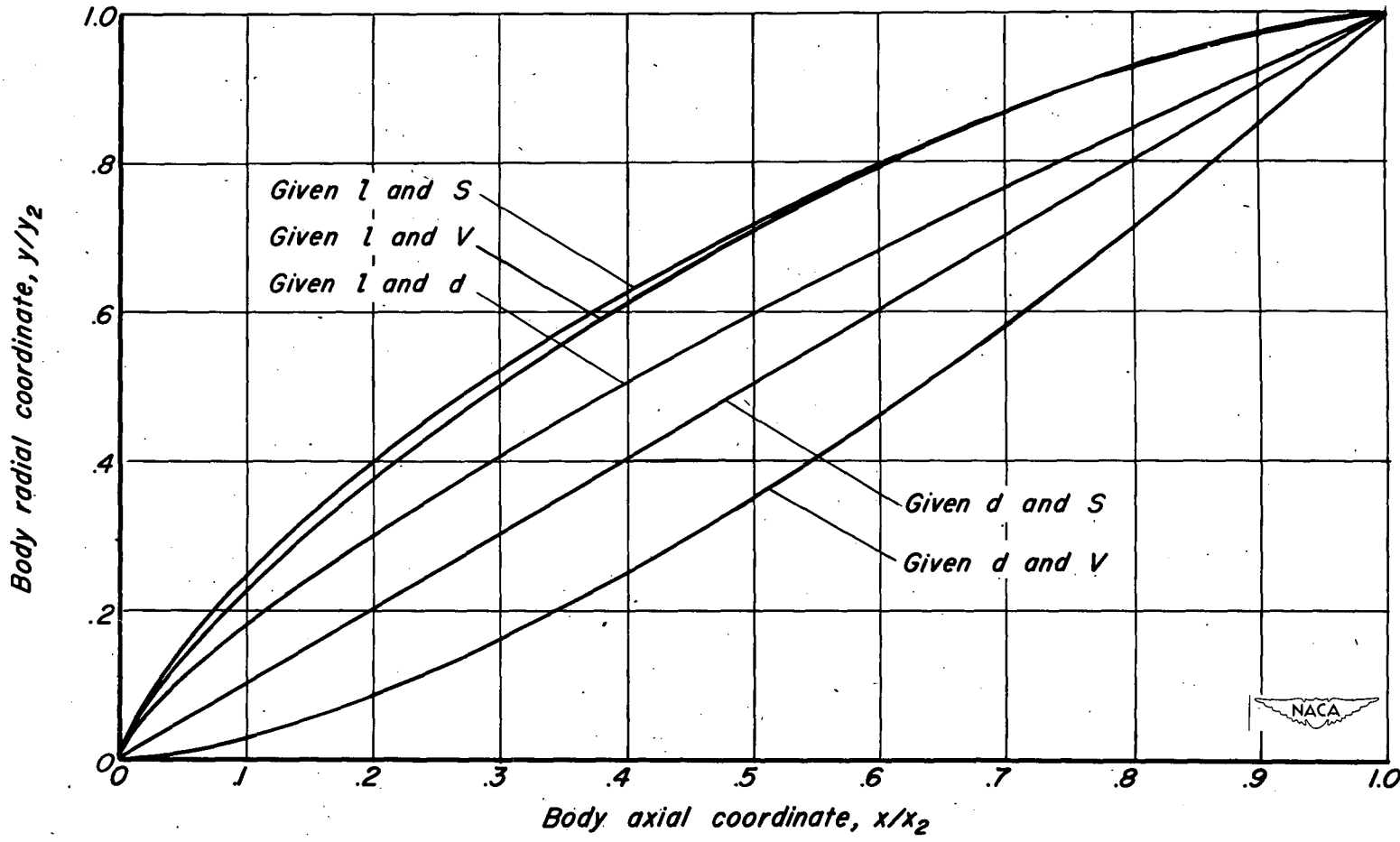


Figure 2.— Minimum drag bodies for various given conditions. ($l/d=5.0$ for all bodies)

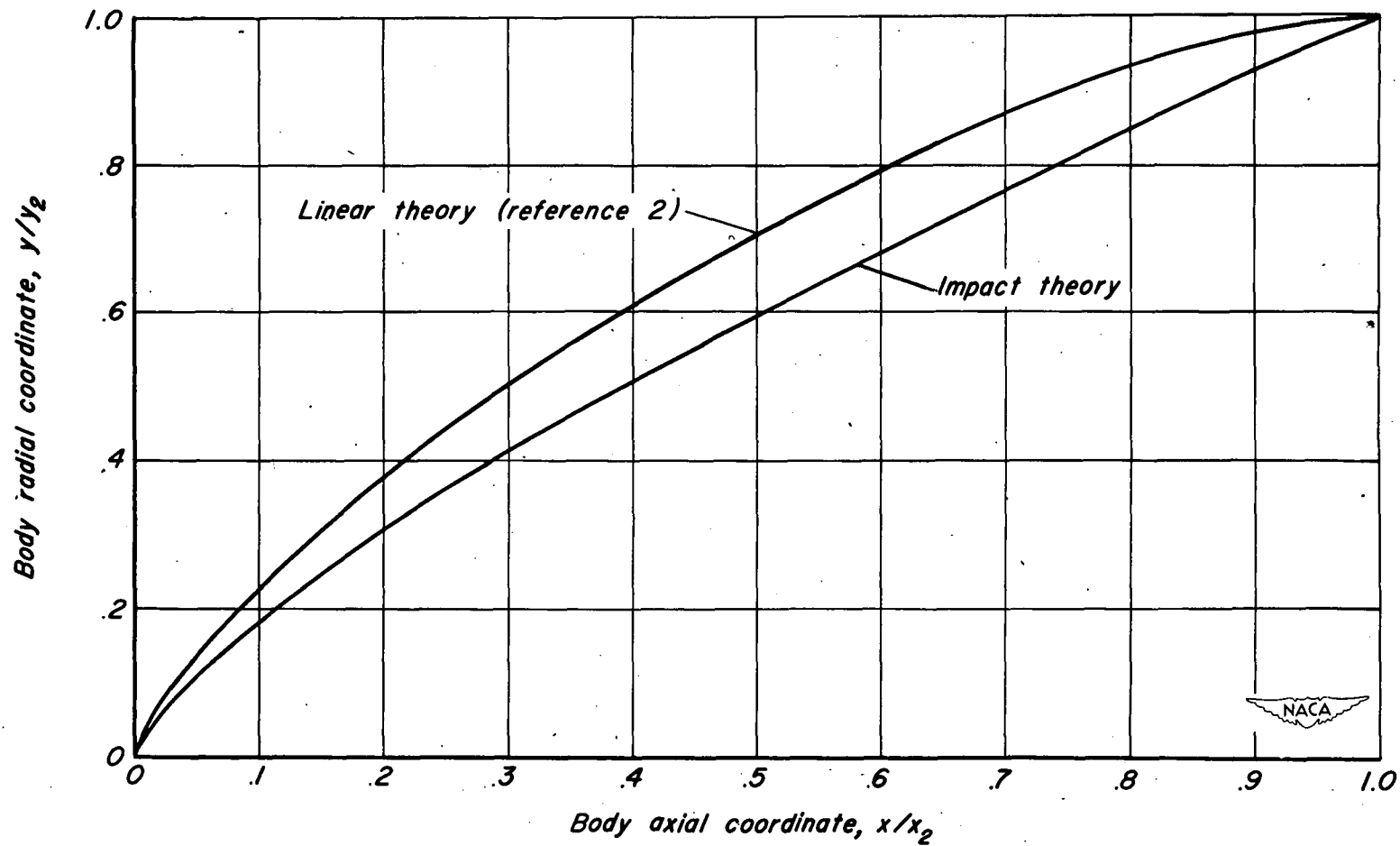


Figure 3.—Comparison of minimum drag bodies of given length and base diameter determined by linear theory and by impact theory.

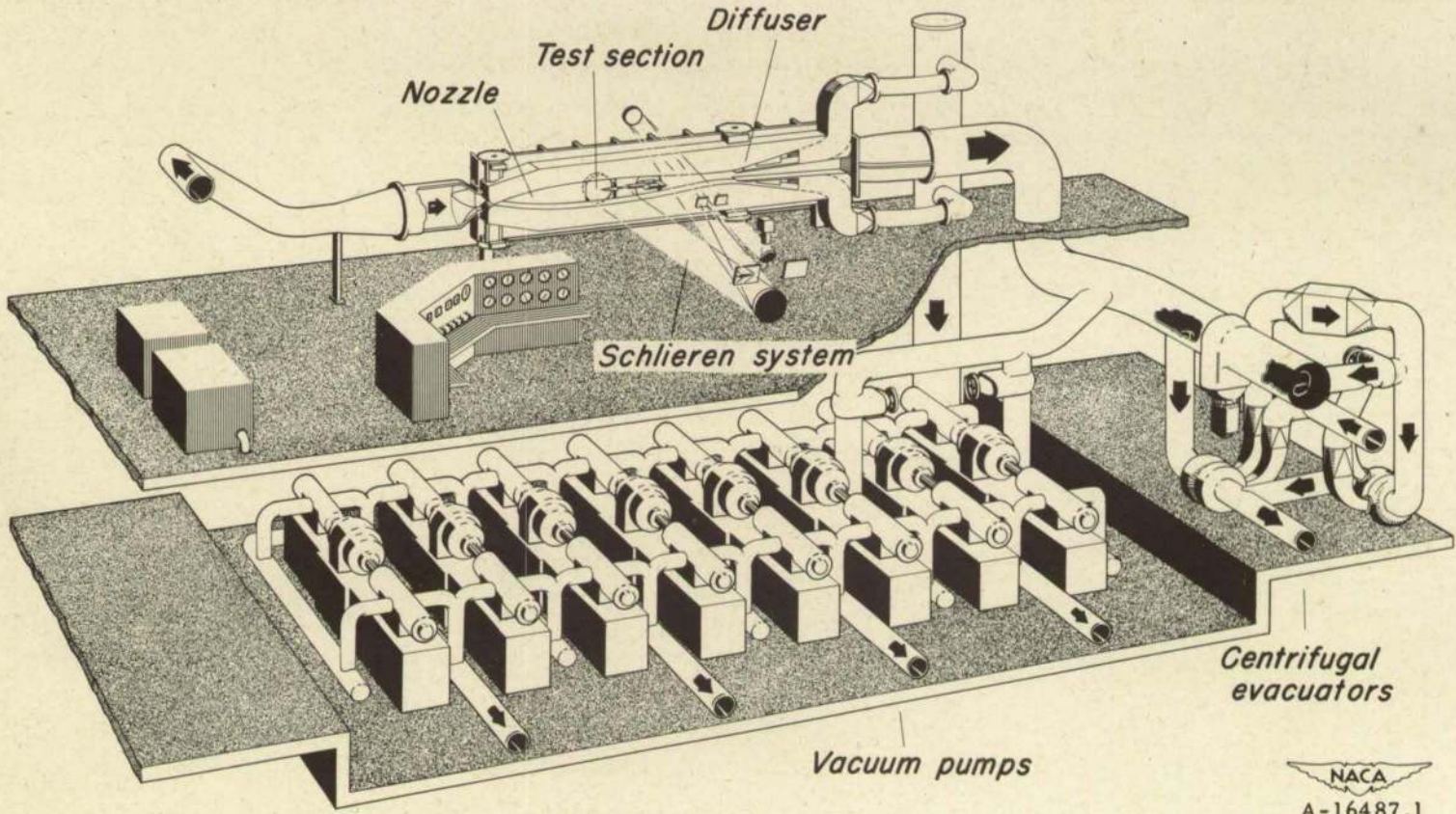


Figure 4.- Schematic view of the 10- by 14-inch Supersonic Wind Tunnel.

NACA
A-16487.1

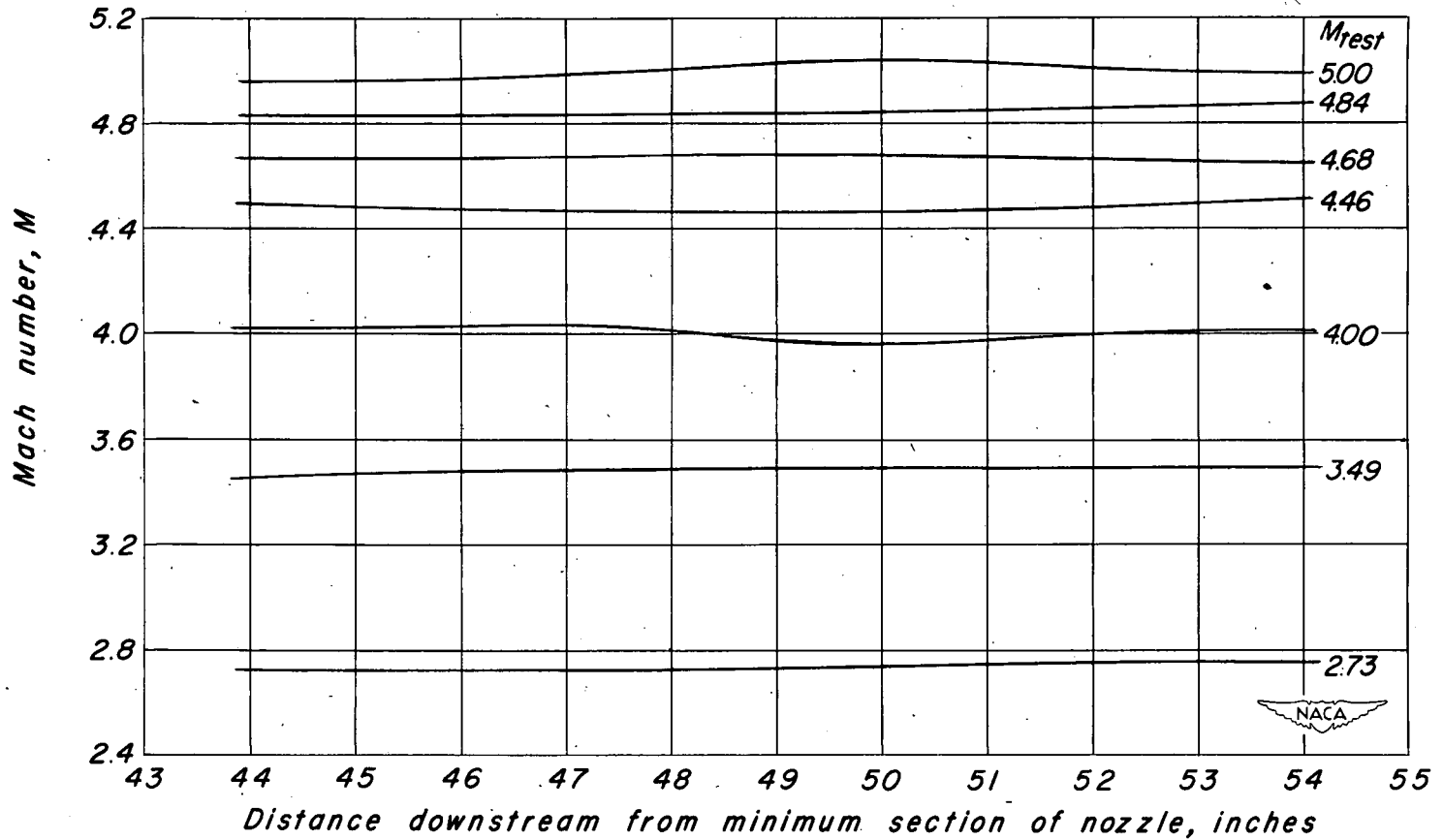


Figure 5.—Mach number distributions on the center line of the 10-by-14-inch Supersonic Wind Tunnel.

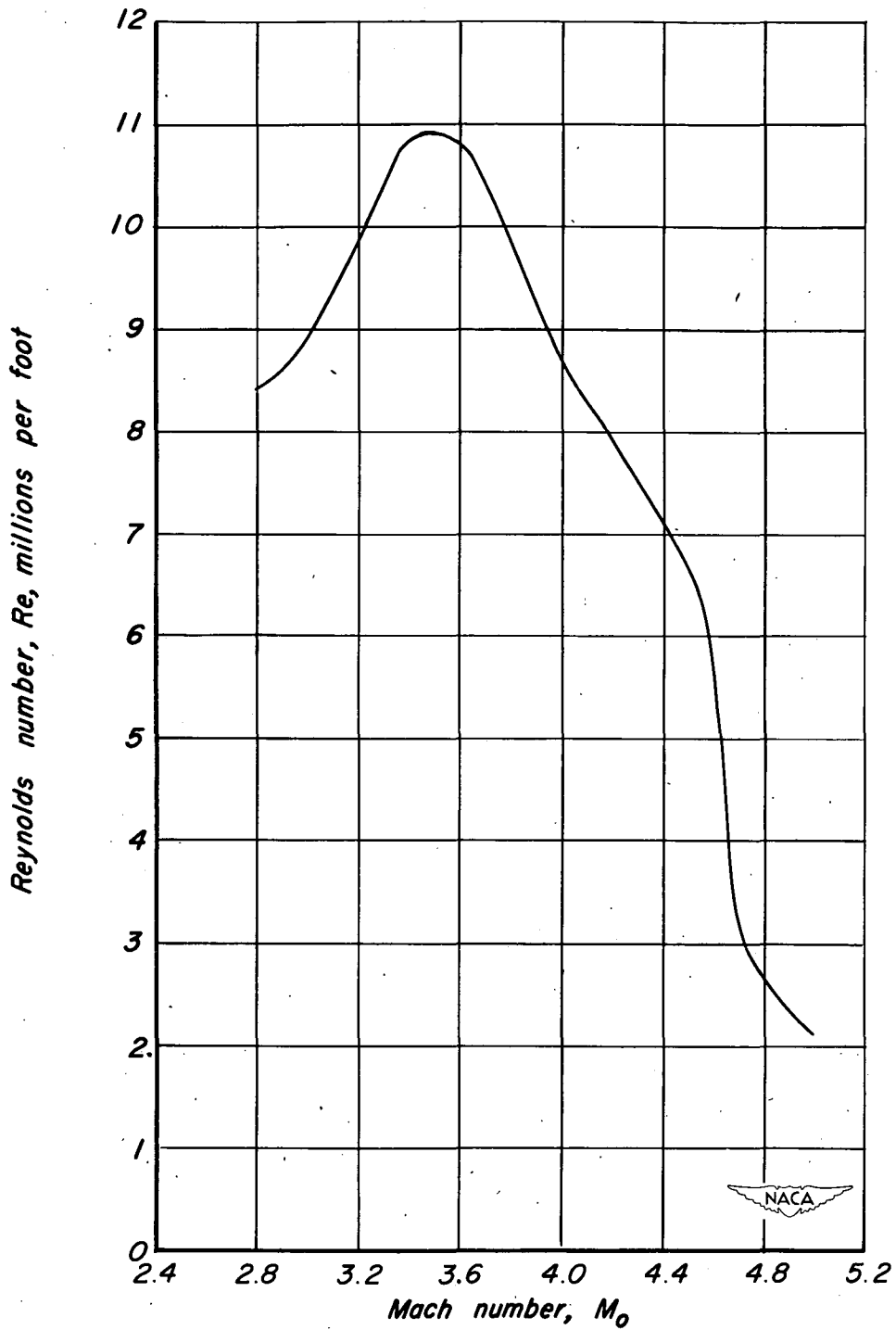


Figure 6.—Variation with Mach number of Reynolds number per foot in the 10-by 14- inch Supersonic Wind Tunnel.

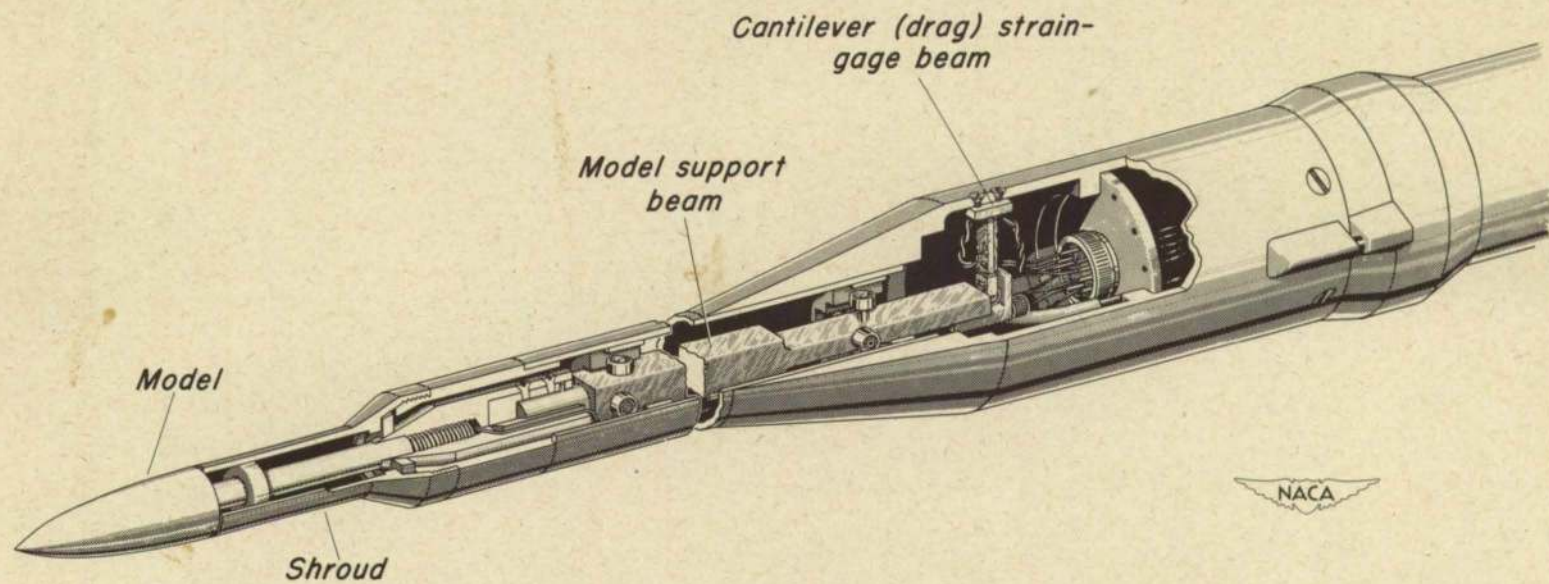


Figure 7.- Cutaway view of the drag balance used in the present tests.

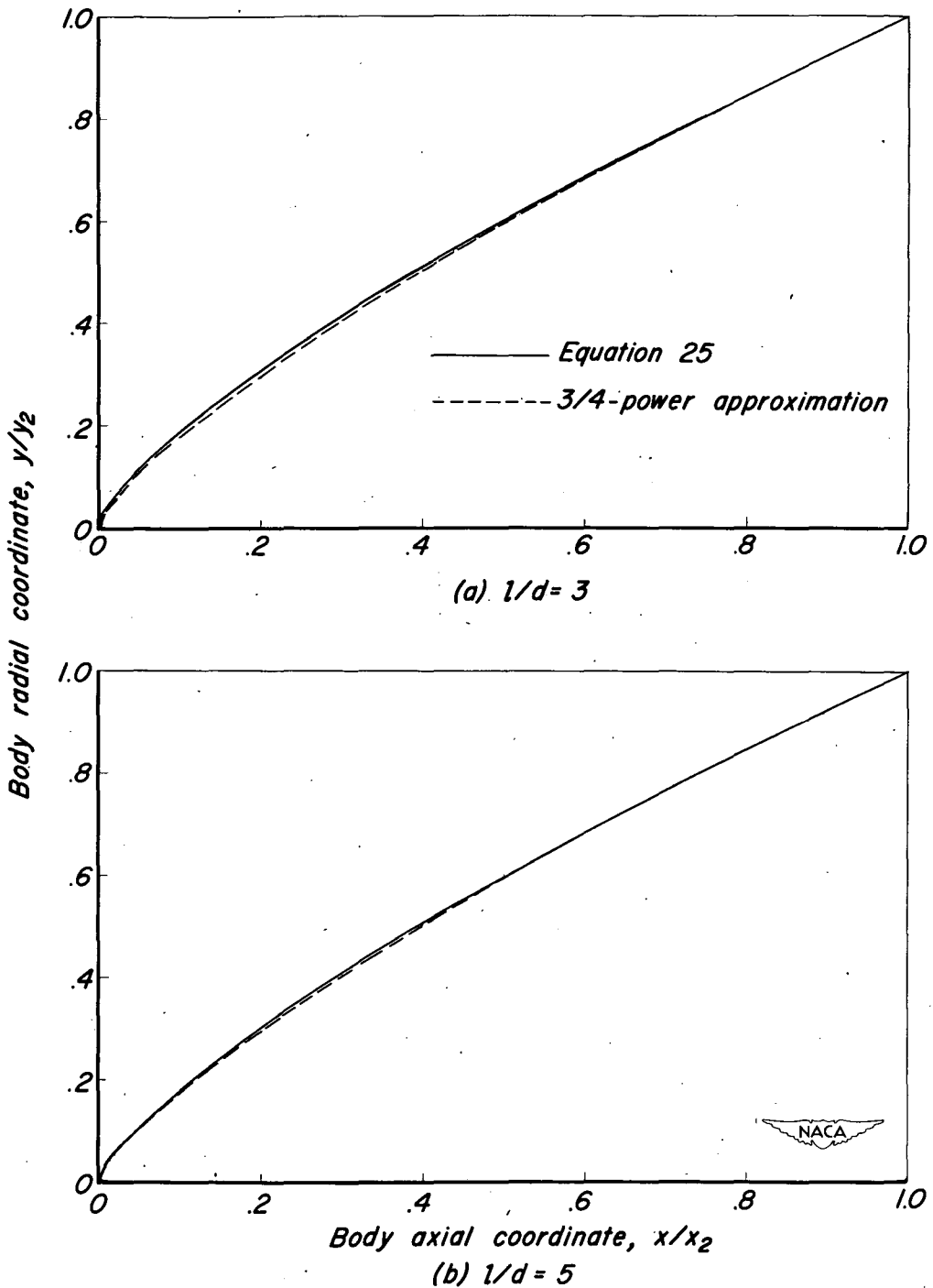
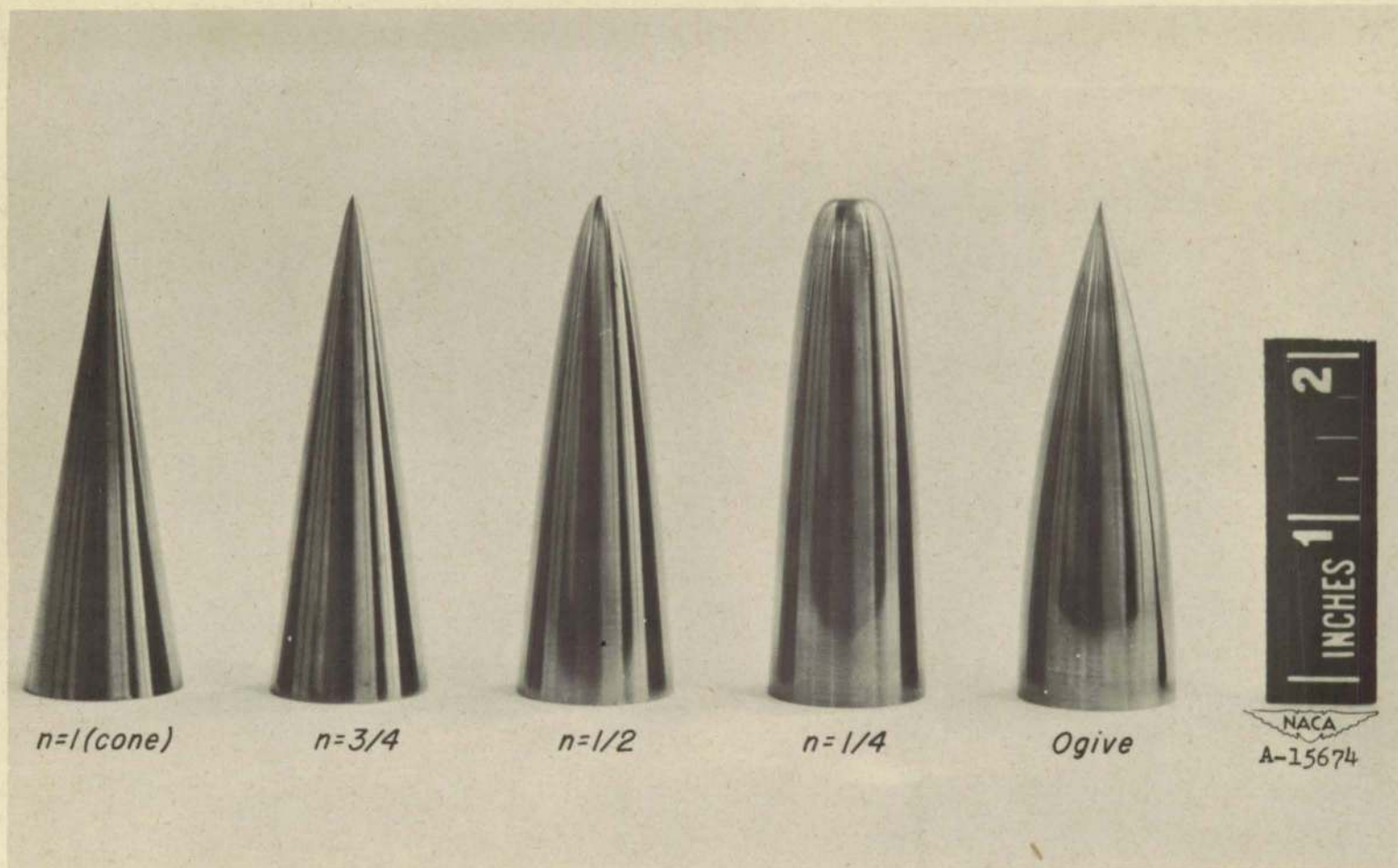


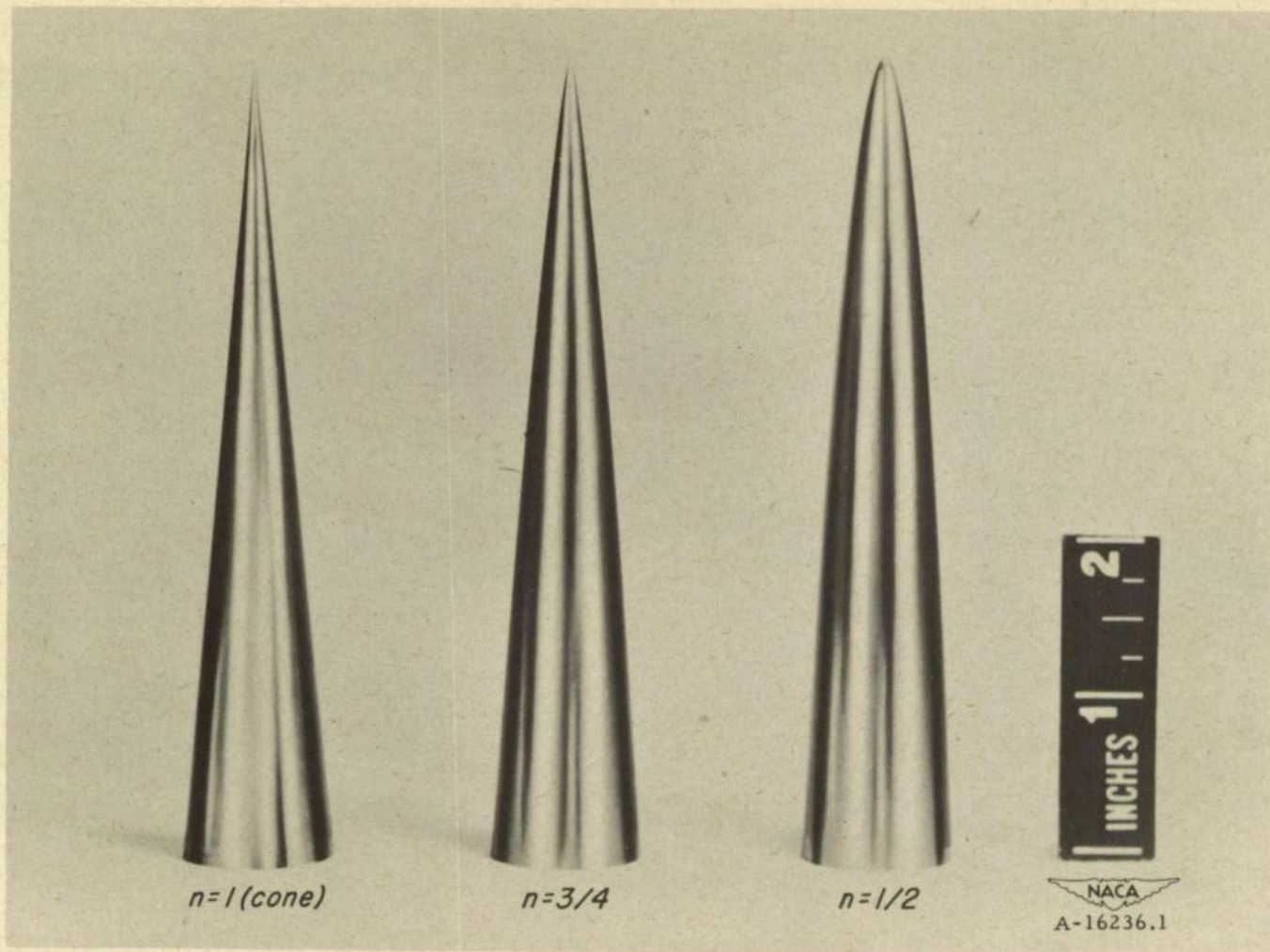
Figure 8. - Comparison of profiles of minimum drag bodies of revolution for given lengths and base diameters with the approximate profiles employed in the present tests.



(a) Fineness ratio 3 bodies.

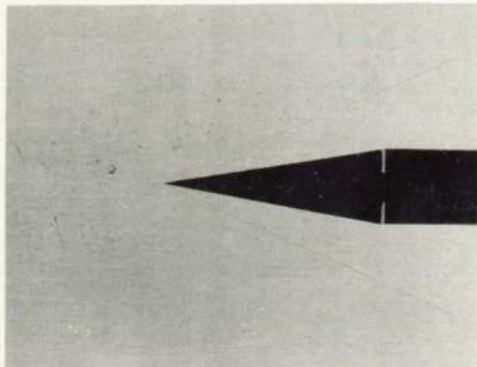
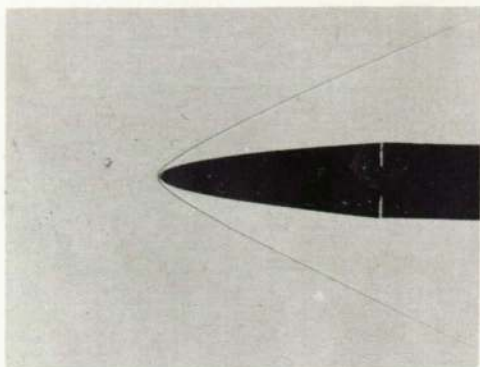
Figure 9.- Photographs of the seven test bodies, the shapes of which are given by the equation

$$y = \frac{d}{2} (x/l)^n, \text{ and the } l/d = 3 \text{ tangent ogive.}$$

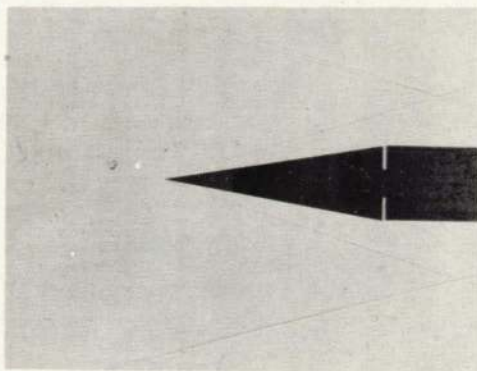
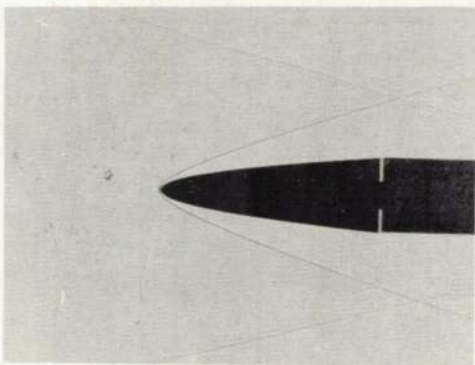


(b) Fineness ratio 5 bodies.

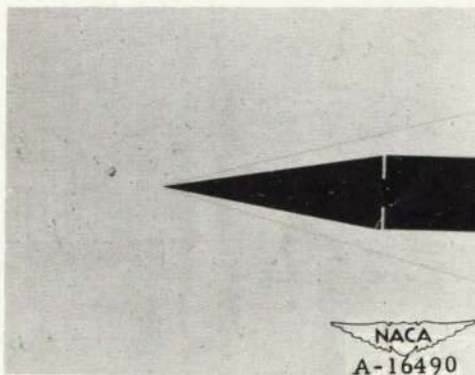
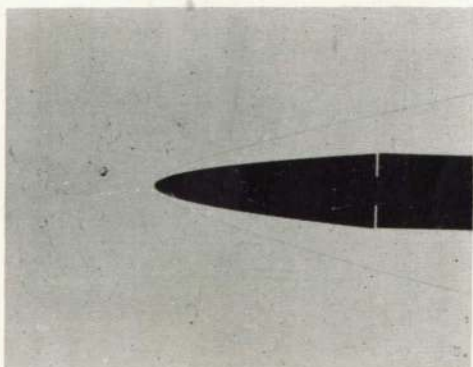
Figure 9.- Concluded.



$M_0 = 2.73$



$M_0 = 4.01$



(a) $l/d = 3$ parabola $M_0 = 5.00$

(b) $l/d = 3$ cone

Figure 10.- Shadowgraphs of fineness ratio 3 conical and parabolic bodies at Mach numbers 2.73, 4.01, and 5.00 in the Ames 10- by 14-inch Supersonic Wind Tunnel.

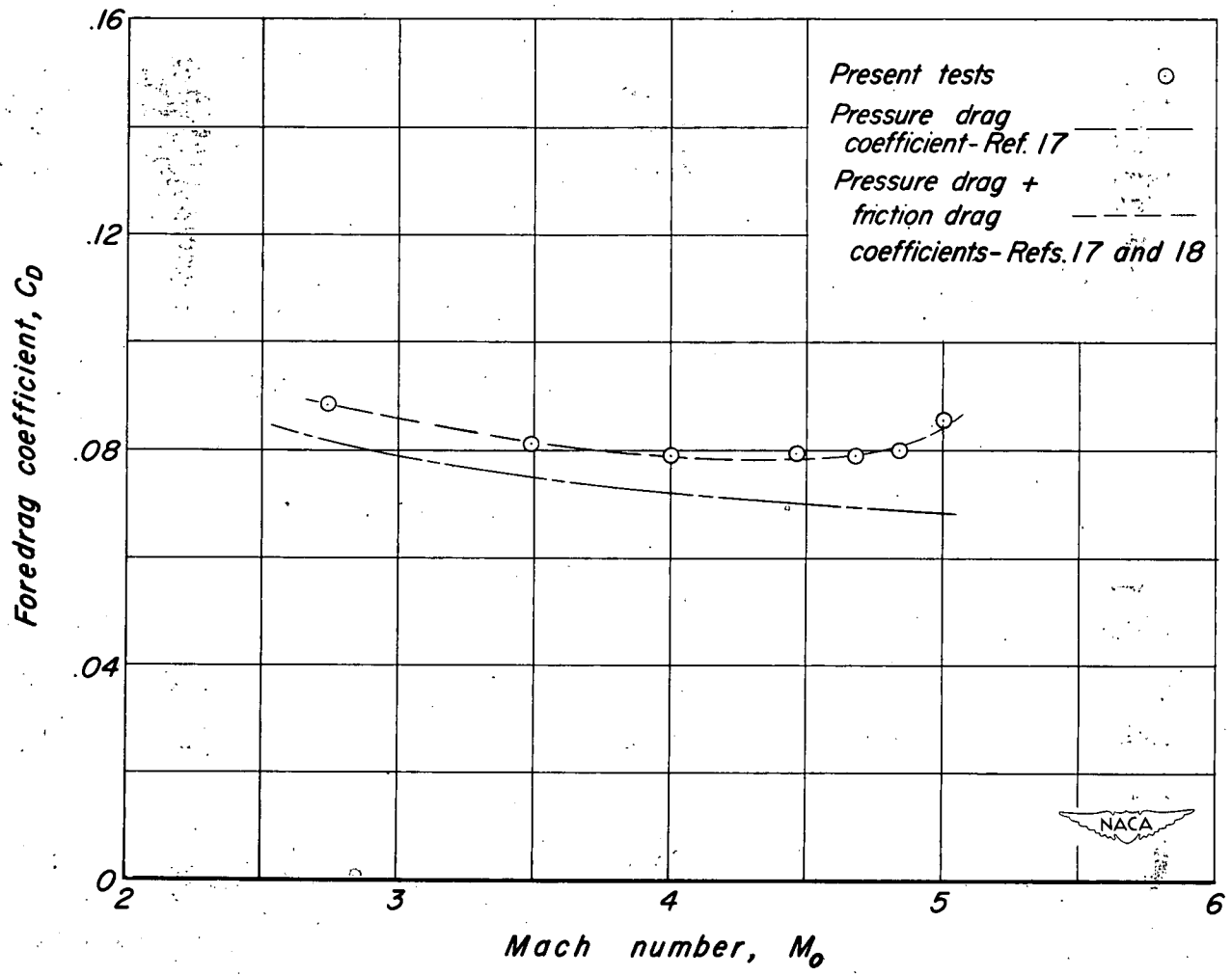


Figure 11. —The variation with Mach number of the foredrag coefficient at zero lift of the $1/d=3$ cone.

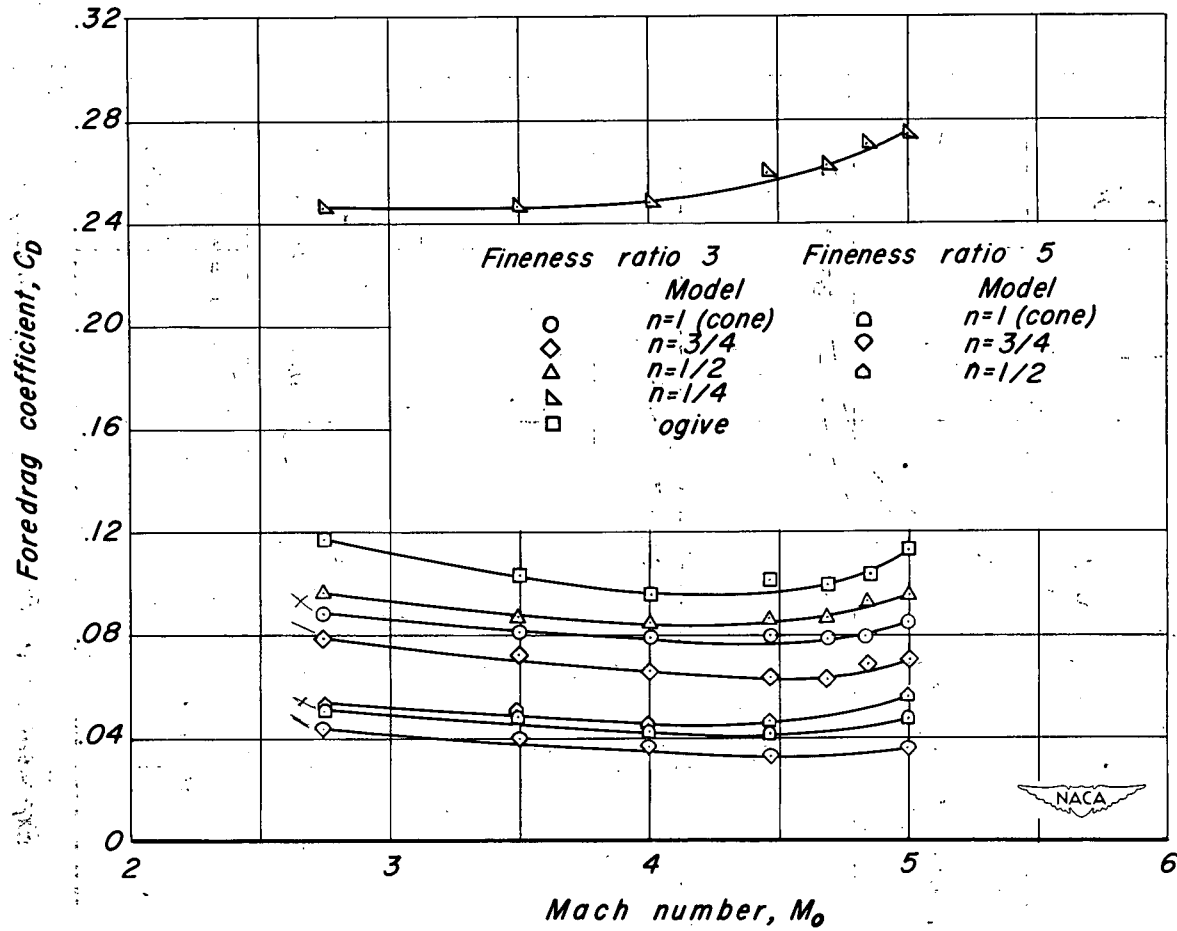
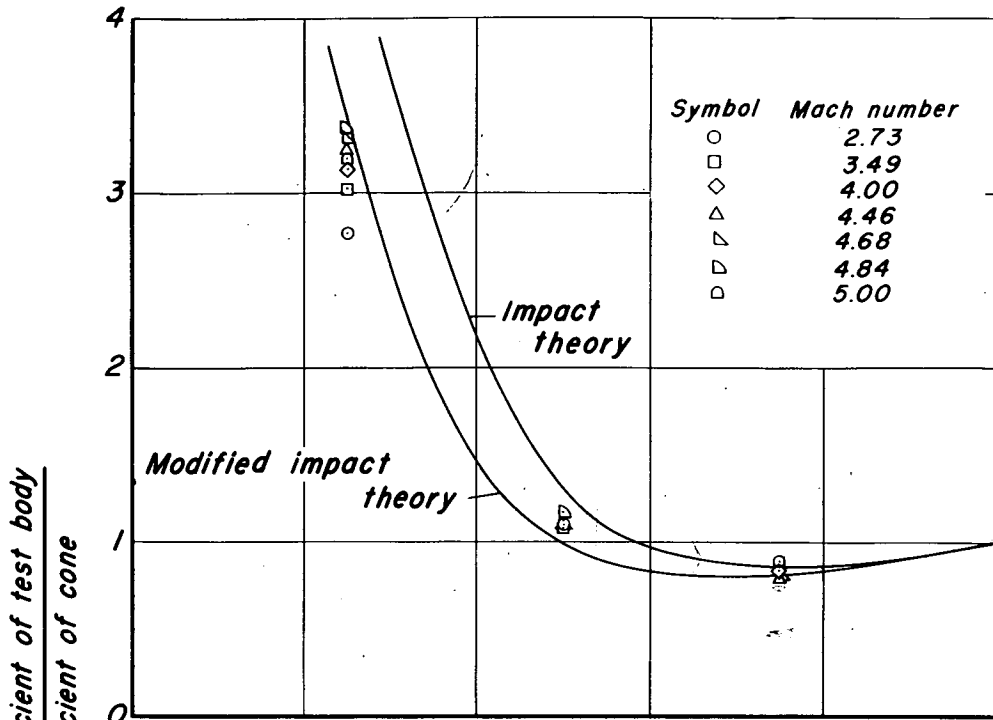
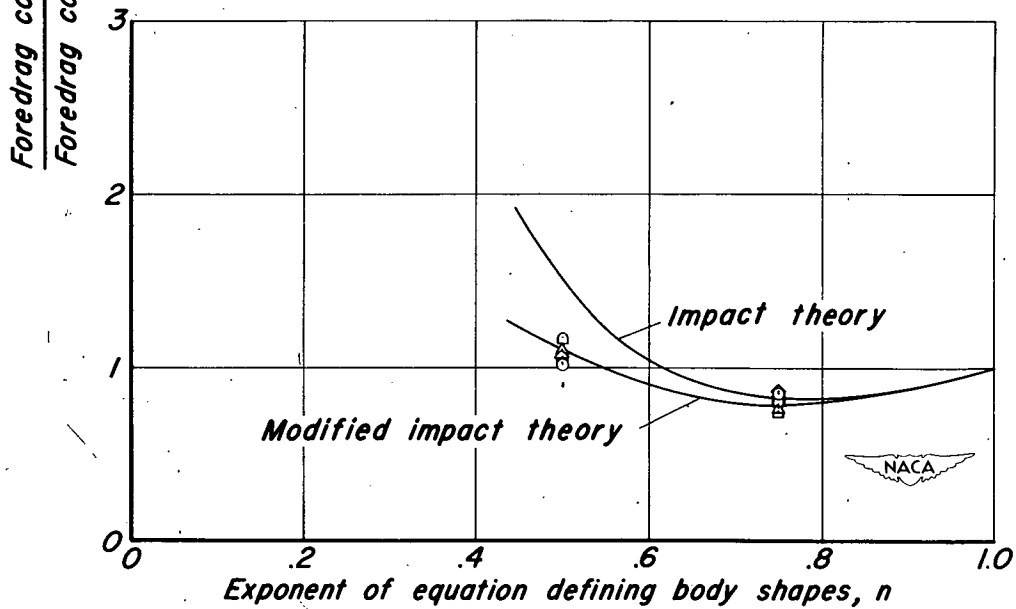


Figure 12. - The variation with Mach number of the foredrag coefficients at zero lift of the test bodies.



(a) $1/d=3$ bodies



(b) $1/d=5$ bodies

Figure 13.- The ratios of foredrag coefficients of test bodies to foredrag coefficients of cones as functions of the exponent, n , in the equation defining body shapes.

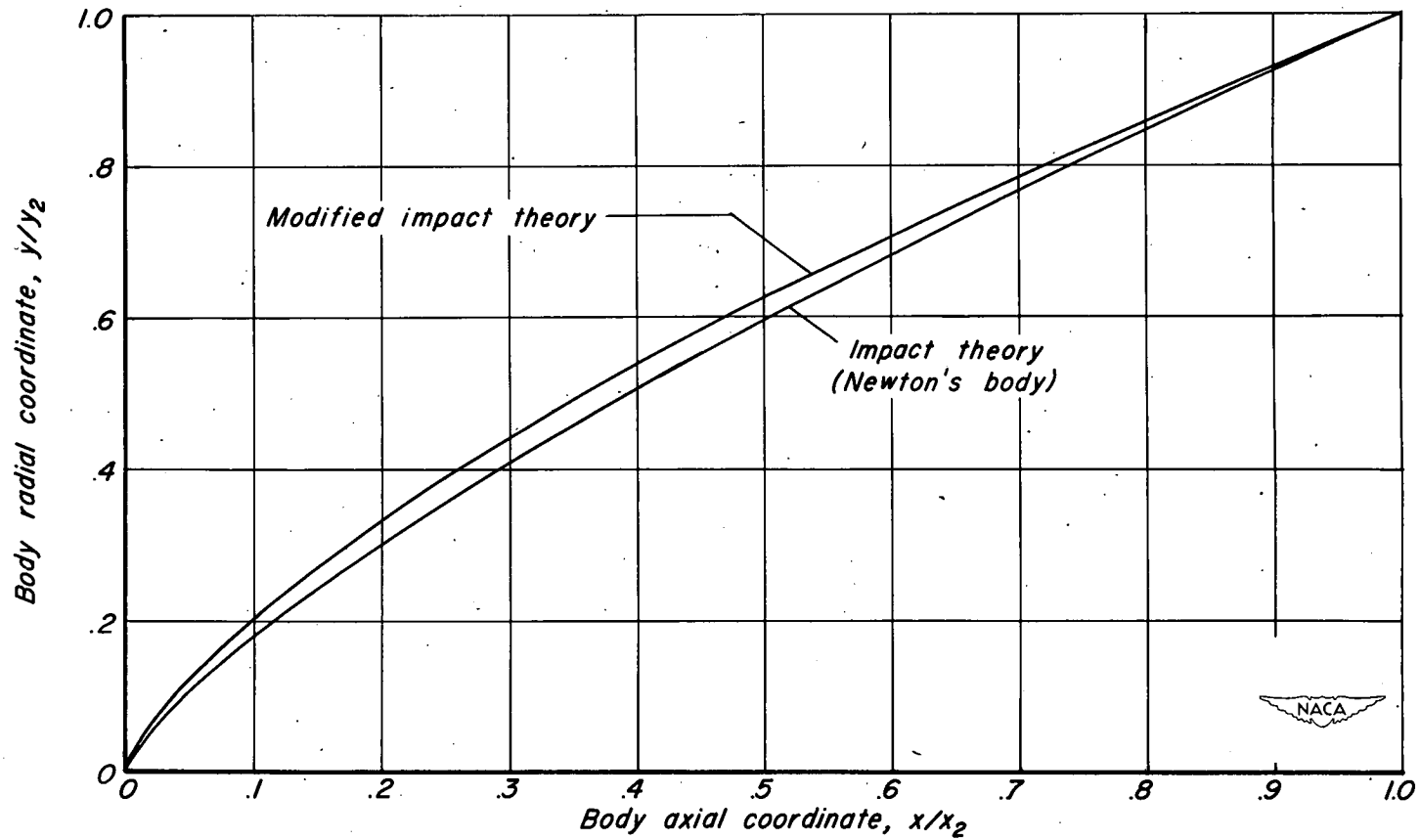


Figure 14.—The effect of centrifugal forces on the shape of the minimum drag body of given length and base diameter. ($l/d=6.18$)

~~CONFIDENTIAL INFORMATION~~

~~CONFIDENTIAL~~

~~CONFIDENTIAL~~